

https://dspace.org/

An approximation to the Heidler Function with an analytical integral for engineering applications using lightning currents

Terespolsky, Brett Ryan

2015

http://hdl.handle.net/10539/22605

Terespolsky, Brett Ryan (2015) An approximation to the Heidler Function with an analytical integral for engineering applications using lightning currents, University of the Witwatersrand, Johannesburg, <http://hdl.handle.net/10539/22605>

Downloaded from a DSpace repository. https://dspace.org/

University of the Witwatersrand,
Johannesburg

Masters Dissertation

An Approximation to the Heidler Function with an Analytical Integral for Engineering Applications Using Lightning Currents

Author:
Brett Ryan Terespolsky

Supervisor:
Prof. Ken. J. Nixon

A dissertation submitted to the Faculty of Engineering and the Built Environment, University of the Witwatersrand, Johannesburg, in fulfilment of the requirements for the degree of Master of Science in Engineering

in the

Lightning and EMC Research Group
School of Electrical and Information Engineering

September 2015

Declaration of Authorship

I, Brett Ryan Terespolsky, declare that this dissertation titled, 'An Approximation to the Heidler Function with an Analytical Integral for Engineering Applications Using Lightning Currents' is my own unaided work. It is being submitted to the Degree of Master of Science to the University of the Witwatersrand, Johannesburg. It has not been submitted before for any degree or examination to any other University.

Signed: _____

Date: _____

"Give me six hours to chop down a tree and I will spend the first four sharpening the axe."

Abraham Lincoln

UNIVERSITY OF THE WITWATERSRAND, JOHANNESBURG

Abstract

Faculty of Engineering and the Built Environment
School of Electrical and Information Engineering

Master of Science in Engineering

by Brett Ryan Terespolsky

The work presented contributes to research in lightning protection simulations and focuses on approximating the Heidler function with an analytical integral and hence a frequency domain representation. The integral of lightning current models is required in the analysis of lightning events including the induced effects and frequency analyses of lightning strikes. Previous work in this area has produced very specific forms of the Heidler function that are used to represent lightning current waveshapes. This work however focuses on a generic solution with parameters that can be modified to produce any lightning current waveshape that is required. In the research presented, such an approximation is obtained. This function has an analytical solution to the integral and hence can be completely represented in the frequency domain. This allows for a true representation of Maxwell's equations for Electromagnetic (EM) fields and for an analytical frequency domain analysis. It has parameters that can be changed to obtain different waveshapes (10/350, 0.25/100, etc.). The characteristics of the approximation are compared with those of the Heidler function to ascertain whether or not the function is applicable for use with the lightning protection standard (IEC 62305-1). It is shown that the approximation does represent the same characteristics as those of the Heidler function and hence can be used in IEC 62305-1 standardised applications. This represents a valuable contribution to engineers working in the field of lightning protection, specifically simulation models.

Acknowledgements

I would like to thank Professor Ken J. Nixon for all his guidance, advice and enthusiasm throughout the duration of this work. I would also like to thank Professor Ian R. Jandrell for his support.

Thank you to my colleagues in the High Voltage and Lightning EMC research group as well as the staff of the Genmin Laboratories for their encouragement and support.

Thanks to the staff and postgraduate students of the school of electrical and information engineering in particular Mr Carson McAfee, Mr Jacques Naudé, Professor Ivan Hofsajer and Ms Yu-Chieh (Jessie) Liu for their long conversations and advice.

Special thanks are extended to Professor Montaz Ali and Professor Anne Love for the advice regarding complicated mathematics.

The following organisations are gratefully acknowledged for funding and supporting the High Voltage and Lightning EMC Research Groups:

- CBI-Electric for direct support and funding the Chair of Lightning at the University of the Witwatersrand.
- Eskom through the Tertiary Education Support Programme (TESP).
- The National Research Foundation (NRF).
- The Department of Trade and Industry (DTI) for Technology and Human Resources for Industry Programme (THRIP) funding.

Furthermore, I formally acknowledge the funding that I received from the following establishments over the years:

- The National Research Foundation (NRF) (*opinions expressed and conclusions arrived at in this thesis are my own and should not necessarily be attributed to the NRF*).
- The University Postgraduate Merit Award.

Last but not least, I am thankful to all my family and friends for their encouragement, patience and support (and to those that assisted in the pain-staking process of proof reading).

Contents

Declaration of Authorship **i**

Abstract **iii**

Acknowledgements **iv**

Contents **v**

List of Figures **ix**

List of Tables **xi**

Symbols **xii**

Nomenclature **xiv**

1 Introduction **1**

2 Approach Taken **3**

2.1 Problem Statement 3

2.2 Contribution of this Dissertation 4

2.3 Scope and Limitations 4

2.4 Methodology of the Study 4

2.5 Conclusion 5

3 Background **6**

3.1 Overview 6

3.2 Application for Lightning Current Models 7

3.2.1 Current Path Analyses 7

3.2.2 Frequency Components of Lightning Currents 9

3.3 IEC 62305-1 - Lightning Protection Standard 9

3.4 Current Waveshape Models 10

3.4.1 The Double Exponential Model 11

3.4.2 The Heidler Function 11

3.5 Heidler Function Approximations 12

3.6 Conclusion 13

4 Heidler Function Approximation **14**

4.1 Overview 14

4.2 Decomposing the Heidler Function 14

4.2.1 Heidler Rise Function 15

4.2.2 Heidler Fall Function 17

4.3 Developing an Approximation to the Heidler Function 18

4.4 Function Definition and Properties 19

4.4.1 Steepness Factor 20

4.4.2 Rise Time Constant 22

4.4.3 Fall Time Constant 23

4.5 Time Domain Properties 25

4.5.1 Derivative 25

4.5.2 Integral 25

4.6 Frequency Domain Properties 26

4.7 Conclusion 27

5 Results: A Comparison to the Heidler Function 28

5.1 Overview 28

5.2 Experimental Methodology 29

5.3 First Short Stroke (10/350) 30

5.4 Subsequent Short Stroke (0.25/100) 33

5.5 Conclusion 35

6 Discussion and Further Work 36

6.1 Overview 36

6.2 Time Domain 36

6.2.1 Lightning Stroke Current 37

6.2.2 Lightning Stroke Current Derivative 40

6.3 Frequency Domain 41

6.4 Further Work 42

6.5 Conclusion 43

7 Conclusion 44

A Approximation to the Heidler Function - Development 46

A.1 Overview 46

A.2 Developing the Approximation 46

A.3 Conclusion 48

B Initial Findings Using the Approximation **49**

B.1 Preamble 49

B.2 Paper Description 49

References **55**

Bibliography **59**

List of Figures

3.1 (a) Physical and (b) Transmission Line models of a lightning strike close to a transmission line that induces over-voltages on the line. 7

3.2 Definitions of short stroke parameters adapted from [1] 10

4.1 Graph depicting the Heidler function in the form of a 10/350 lightning waveform with a 200 kA peak. 15

4.2 Graph depicting the rise function of the Heidler function (an S-curve). . . 16

4.3 Graph depicting the decay function of the Heidler function (exponential decay function). 17

4.4 Graph depicting the rise function of the approximation function (an S-curve). 19

4.5 Graph of an example Heidler function approximation lightning current waveshape in the form of a 10/350 with a 200 kA peak current. 20

4.6 Graph showing the effect of changing the steepness factor (n_a) in the approximation function while keeping all the other variables constant. . . 21

4.7 Graph showing the effect of changing the rise time constant (ω_0) in the approximation function while keeping all the other variables constant. . . 23

4.8 Graph showing the effect of changing the fall time constant (τ_2) in the approximation function while keeping all the other variables constant. . . 24

4.9 Graph showing the derivative of the approximation function shown in *Figure 4.5*. 26

4.10 Amplitude density of the approximation model produced from the waveshape plotted in *Figure 4.5*. 27

5.1 Graph of the first short stroke (10/350) current model using both the Heidler function and the approximation. The time scale is up to 200 μs and the amplitude is as high as 210 kA. 30

5.2 Graph of the first time derivative of the first short stroke (10/350) current model using both the Heidler function and the approximation. The time scale is up to 200 μs and the amplitude is as high as 30 kA/μs. 32

5.3 Current density of the approximation model produced from the waveshape plotted in *Figure 5.1*. 32

5.4 Graph of a subsequent short stroke (0.25/100) current model using both the Heidler function and the approximation. The time scale is up to 5 μs and the amplitude is as high as 52 kA. 33

5.5 Graph of the first time derivative of a subsequent short stroke current model using both the Heidler function and the approximation. The time scale is up to 5 μs and the amplitude is as high as 300 kA/μs. 34

5.6 Current density of the approximation model produced from the waveshape plotted in *Figure 5.4*. 35

6.1 Effects of varying the steepness factors, n_h and n_a, in both the Heidler function and the approximation respectively. The (a) Heidler function and the (b) Heidler function derivative are compared to the (c) approximation and its (d) derivative. 39

6.2 Effects of varying the rise time constants, τ_1 and ω_0, in both the Heidler function and the approximation respectively. The (a) Heidler function and the (b) Heidler function derivative are compared to the (c) approximation and its (d) derivative. 40

6.3 Amplitude densities of the different lightning currents according to Lightning Protection Level (LPL)-I as stipulated by the IEC 62305-1 with the results of the Fourier transform of the approximation (adapted from Figure B.5 in [1]). The numbers point to the solid lines obtained from the standard. 42

A.1 Graph depicting the rise function of the Heidler function (an S-curve). . . 47

List of Tables

4.1 Constant values used in *Equation 4.9* to obtain the graphs plotted in *Figure 4.6* 21

4.2 Variation of rise time and peak current of the approximation with a change in the steepness factor (n_a) as a percentage of a 200 kA 10/350 waveshape. 22

4.3 Constant values used in *Equation 4.9* to obtain the graphs plotted in *Figure 4.7* 22

4.4 Variation of rise time and peak current of the approximation with a change in the rise time constant (ω_0) as a percentage of a 200 kA 10/350 waveshape. 23

4.5 Constant values used in *Equation 4.9* to obtain the graphs in *Figure 4.8* . 24

4.6 Variation of rise time and peak current of the approximation with a change in the fall time constant (τ_2) as a percentage of a 200 kA 10/350 waveshape. 25

5.1 Parameters used in *Equations 3.5* and *4.9* to plot the waveshapes shown in *Figure 5.1.* 30

5.2 Parameters used in *Equations 3.5* and *4.9* to plot the waveshapes shown in *Figure 5.4.* 34

6.1 Comparison of the errors for the approximation and the Heilder function for both the first and subsequent strokes 38

Symbols

Electromagnetic Equations of a Lightning Stroke

$E_z(D,t)$	Electric field	V/m
$B_\phi(D,t)$	Magnetic field	T

Lightning Current Return Stroke Modelling

$i(z',t)$	Lightning current return stroke model	A
$i(0,t)$	Lightning channel base current	A

Double Exponential Function

$i_e(t)$	Double exponential lightning stroke current model	A
I_0	Peak current	A
A	Double exponential peak current correction	
α	Double exponential decay time constant	1/s
β	Double exponential rise time constant	1/s

Heidler Function

$i_h(t)$	Heidler function lightning stroke current model	A
η	Peak current correction	
τ_1	Heidler rise time constant	s
τ_2	Decay time constant	s
n_h	Heidler steepness factor	
$i'_h(t)$	First time derivative of $i_h(t)$	A/s
$x_h(t)$	Heidler function rise time function	
$y(t)$	Decay function	

Heidler Function Approximation

$X_a(s)$	Rise time function of the approximation (Laplace domain)	
$x_a(t)$	Rise time function of the approximation (time domain)	
$i_a(t)$	Approximated lightning stroke current model	A
ω_0	Rise time constant of the approximation	rad/s
n_a	Steepness factor of the approximation	
$i'_a(t)$	First time derivative of $i_a(t)$	A/s
$I_a(j\omega)$	Fourier transform (angular frequency) of $i_a(t)$	
$I_a(jf)$	Fourier transform (linear frequency) of $i_a(t)$	A/Hz

Error Evaluation

$e(s)$	Error function	A
$e'(t)$	First time derivative of $e(t)$	A/s

Nomenclature

Decay time constant	A constant that is used to change the decay time (the time to 50% of peak current) of the lightning current waveshape.
Decay time function	The function that dictates what the shape of the decay of the waveshape is.
First short stroke	A short stroke that is defined by the IEC 62305-1 as having a rise time of 10 μs and a decay time of 350 μs.
Heidler function	A function used to model lightning impulse currents. There are several parameters that can be changed to manipulate the rise and fall times of the waveshape. This function is stipulated in the IEC 62305-1 standard as the standardised lightning impulse current model used for Lightning Protection System design.
Heidler function approximation	The function developed in this dissertation that approximates the Heidler function with an analytical integral.
IEC 62305	The IEC lightning protection standard.

IEC 62305-1	Part one of the IEC 62305. This details all the parameters of lightning currents and the nomenclature used in lightning current models. This standard also details the first and subsequent short strokes and how they can be simulated using the Heidler function.
Lightning stroke model	A mathematical model used to represent a lightning current waveshape. Examples of these are the Heidler function, the double exponential function and the approximation to the Heidler function that is represented in this dissertation.
Rise time constant	A constant that is used to change the rise time of the lightning current waveshape.
Rise time function	The function that dictates what the shape of the rise of the waveshape is.
Short stroke	A component of a lightning stroke that is impulsive in nature unlike the long stroke which is a comparatively long sustained current.
Subsequent short stroke	A short stroke that is defined by the IEC 62305-1 as having a rise time of 0.25 μs and a decay time of 100 μs.
Waveshape	The shape of a graph in the time domain.
Waveshape steepness	A higher steepness in a waveshape results in a larger maximum instantaneous change in current.

To my loving parents
for their endless support
and belief in me.

Моей Шурочке,
за любовь и поддержку

Chapter 1

Introduction

Mathematical lightning current models are used in many areas of research ranging from the design of Lightning Protection Systems (LPSs) to the understanding of electric and magnetic fields associated with lightning discharges [1, 2]. Lightning current models are typically used as design tools and for further research into the understanding of the effects of a lightning strike. The Heidler function, which is the standard lightning current model, cannot be integrated analytically and therefore the frequency domain of the lightning strike cannot be accurately presented nor is it possible to utilise Maxwell's equations in analysing lightning events. This research presents a suitable replacement to the Heidler function for situations where an integral is required.

This replacement falls under the category of an approximation to the Heidler function and as such, it can be tailored to any waveshape required just as the Heidler function can by varying the parameters. An investigation is carried out to determine the accuracy of the approximation. This is done by using computer simulations of the approximation and the results are compared to the Heidler function to determine the viability of this approximation in the design of LPSs. All the results are based on the waveshapes defined in the IEC 62305-1 so that there is a known control[1].

Chapter 2 details the ***approach taken*** in designing and evaluating the approximation to the Heidler function. The assumptions and constraints made in this study are outlined. The significance of this study in the field of lightning research is discussed with reference to the problem statements.

[1] *Note to the reader:* This research assumes familiarity with the IEC 62305-1 standard ("Protection against lightning - Part 1: General principles") - it is advised that the reader have access to this document when reading this dissertation.

Chapter 3 discusses the relevant ***background*** information with respect to this research. This includes information about the different lightning current models and their applications. Key areas relating to this study are detailed from the IEC 62305-1 standard. A review of the existing work in the field of approximating lightning currents is also identified.

Chapter 4 provides the ***approximation to the Heidler function*** that was developed in this study. All the components of the equation are discussed as well as the parameters used to create the various waveshapes. The properties of the approximation along with its derivative and integral are detailed. A comparison of the parameters used in the approximation and the Heidler function are also given.

Chapter 5 investigates the accuracy of the approximation by simulating ***results*** and comparing them to the expected values obtained from the Heidler function. This includes the waveshapes in the IEC 62305-1 standard and the frequency responses.

Chapter 6 summarises the results obtained from the simulations. A ***discussion*** of the viability of this approximation as a suitable replacement to the Heidler function is provided. ***Future work*** in the field of approximating lightning current models is detailed with the goal of optimising the approximation detailed in this study.

Chapter 7 provides a ***conclusion*** to the work and discusses the viability of this function in various fields of lightning research.

Appendix A details the ***development*** of the approximation including all the mathematical steps.

Appendix B presents an edited copy of a paper published at a peer-reviewed conference, to provide the preliminary results obtained using the approximation.

Chapter 2

Approach Taken

An overview of the work addressed in this study is detailed in this chapter. The problem statement, contribution of the dissertation and the methodology of the study are provided. This gives a quick overview of why the study has been undertaken, what it provides and how it was performed and evaluated.

2.1 Problem Statement

The Heidler function was developed to represent any lightning current waveshape for modelling lightning currents in design or analysis [3]. However there is no analytical integral to the Heidler function. This leads to issues when trying to calculate the Electromagnetic (EM) fields produced by a lightning stroke. Moreover, there is no way to analytically calculate the Fourier transform of the Heidler function and hence the frequency components of a lightning stroke. When designing LPSs and/or calculating the induced effects of lightning strikes, there is a need for the analytical integral of the lightning current waveshape.

The IEC 62305-1 standard defines the Heidler function as the standardised lightning current waveshape. As there is no integral to this function, many researchers have used the double exponential function in its place. There are several limitations associated with the double exponential function making it an unsuitable replacement. A key limitation is that there is an instantaneous rise in current at $t = 0$ which is not physically realisable. *Chapter 3* gives a more detailed background into the applications of lightning current models, the IEC 62305-1 and the different lightning models and approximations.

There is a requirement for a function that can be used in place of the Heidler function in the standard. This function should take a similar form to that of the Heidler function, it

should be intuitive when compared to the Heidler function and the mathematics in using this function should be as simple as that of the Heidler function. Most importantly this function must have an analytical integral for lightning current applications.

2.2 Contribution of this Dissertation

This study develops a function that approximates the Heidler function in the time domain. This approximation has the advantage of having an analytical integral and taking the same form as that of the Heidler function; only the parts of the Heidler function that cannot be integrated are replaced in producing this approximation. This approximation is easy to use and the parameters for creating different lightning current waveshapes are determined easily. In a system design or simulation, it would be trivial to replace the Heidler function with this approximation. Most importantly, it can be utilised in performing Maxwell's equations or finding the Fourier transform (frequency components). *Chapter 4* details the development process of this function with its properties.

2.3 Scope and Limitations

The approximation developed in this research has a clearly defined scope: it is based on the waveshapes mentioned in the IEC 62305-1 lightning protection standard. The approximation is ideally suited for use in cases where the integral of the Heidler function is required. Therefore, the IEC 62305-1 standard is used as a starting point for the research which introduces some limitations. For example, the parameters for the various Lightning Protection Levels (LPLs) and lightning current models are dictated by those defined in this standard. The research is limited to the definitions in this standard and comparisons are only made to the two waveshapes mentioned therein. The parameters of the approximation are determined empirically from those defined in the IEC 62305-1 for the Heidler function. No evidence is provided in this research to show that this approximation can be used outside of the bounds of the IEC 62305-1. *Chapter 6* discusses further research that can be carried out to either overcome or verify these limitations.

2.4 Methodology of the Study

This study is performed by evaluating the limitations associated with the Heidler function and devising a solution. The approach taken in developing this approximation is different to the other approximations outlined in *Section 3.5* because the development is done in

the Laplace domain and the inverse Laplace transform is obtained. This is done only for the part of the equation that cannot be integrated. This part of the function is substituted back into the general form of the function to create the overall approximation. This is all discussed in more detail in *Chapter 4*

As this study is the development of an equation, all results are based on simulations of the approximation. In order to determine the accuracy of the approximation, a control is required. The IEC 62305-1 details two waveshapes and gives the corresponding parameters for the Heidler function for these waveshapes. The approximation is simulated alongside these waveshapes and the maximum errors are obtained by calculating the absolute difference between the approximation and the Heidler function. The derivatives are compared in a similar manner. *Chapter 5* details all of the results obtained using this methodology.

Conclusions are drawn about the accuracy of the approximation and the frequency components are plotted as an indication of their similarity to the IEC 62305-1 standard. This is all detailed in *Chapter 6*.

2.5 Conclusion

This chapter has given an overview of the entire study. It has essentially answered the questions of what, why and how relating to the study. It has also given an outline to which chapters answer what questions and how.

The following chapter gives the background that relates to the work done. This is done by detailing some applications of lightning current models, the lightning protection standard, lightning current models and some of the work that has been done in approximating the Heidler function.

Chapter 3

Background

This chapter provides the background knowledge that is required to understand this research and why it was undertaken. Insight is given into the applications of lightning current models, including induced currents on transmission lines and lightning frequency component analyses. The terminology used in the IEC lightning protection standard is defined giving insight into the reason for approximating the Heidler function. The Heidler function and the double exponential function are also defined and discussed. A literature review is carried out showing some of the work done by other researchers in obtaining approximations to the Heidler function.

3.1 Overview

In order to understand the research presented in this dissertation, there are certain concepts that require further description. In the previous chapter the research questions of what, why and how are answered. However, very little detail is given about the concepts and ideas mentioned. This chapter explains a few of the applications where it is appropriate to utilise lightning current models. Key components of the IEC 62305-1 (part one of the lightning protection standard) are explained. Two of the more common lightning current models are detailed and some of the approximations that have been developed by other researchers are detailed. This all gives some background relating to the study.

3.2 Application for Lightning Current Models

There are several instances when there is a requirement to use a lightning current model such as in the design of LPSs. Two of the more specific cases where lightning current models are used are detailed below. These include current path analyses using return stroke modelling and the need for the frequency components of lightning.

3.2.1 Current Path Analyses

Return stroke models are characterised into four primary classes, namely gas dynamics model, electromagnetic model, distributed circuit model and the engineering model [4–6]. The engineering model is the primary model used when looking at induced effects on power lines.

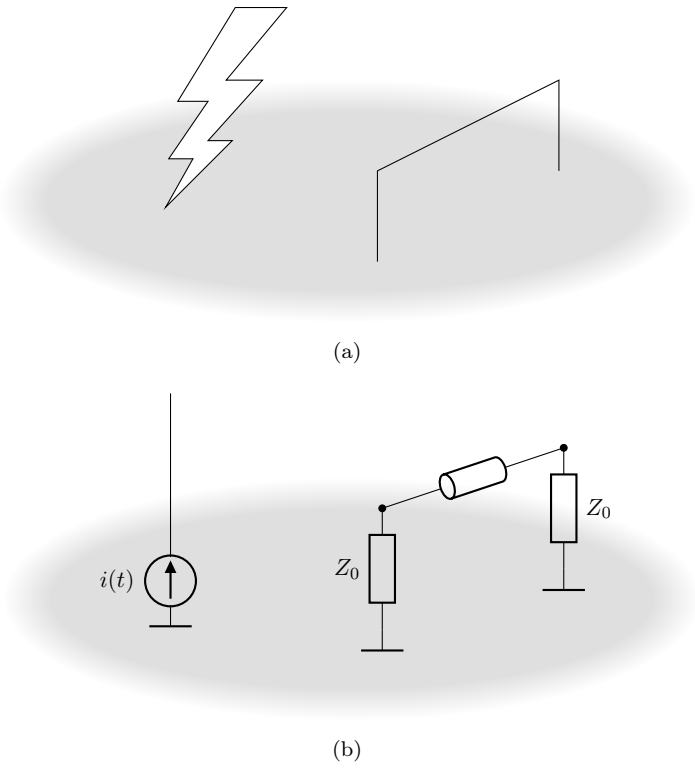


FIGURE 3.1: (a) Physical and (b) Transmission Line models of a lightning strike close to a transmission line that induces over-voltages on the line.

Figure 3.1 shows the (a) physical and (b) return stroke models for a lightning strike in close proximity to a transmission line. From these figures it can be seen that when modelling a lightning strike occurring in close proximity to a transmission line, the lightning channel is modelled as a monopole with a perfectly conductive ground and a vertical current path [4, 7, 8].

Information about the EM fields are required when calculating the induced effects of the lightning strike on the transmission line. The induced currents can be calculated by integrating the different components of the EM fields as outlined by Agrawal et al. [9]. The Lightning Electromagnetic Pulse (LEMP) equations need to be determined before calculating the EM fields. The equations for the EM fields can be seen in *Equations 3.1* and *3.2* respectively. These are defined by Uman et al. as the LEMP equations [10].

$$E_z\left(D,t\right) = \frac{1}{2\pi\epsilon_0}\left[\int_0^H \frac{2-3\sin^2\theta}{R^3} \times \int_0^t i\left(z,\tau-\frac{R}{c}\right)\,d\tau dz + \int_0^H \frac{2-3\sin^2\theta}{cR^2} i\left(z,t-\frac{R}{c}\right)\,dz - \int_0^H \frac{\sin^2\theta}{c^2R}\frac{\partial i\left(z,t-\frac{R}{c}\right)}{\partial t}\,dz\right] \tag{3.1}$$

$$B_\phi\left(D,t\right) = \frac{\mu_0}{2\pi}\int_0^H \frac{\sin\theta}{R^2} i\left(z,t-\frac{r}{c}\right)\,dz + \frac{\mu_0}{2\pi}\int_0^H \frac{\sin\theta}{cR}\frac{\partial i\left(z,t-\frac{R}{c}\right)}{\partial t}\,dz \tag{3.2}$$

The full extent of what these equations mean is beyond the scope of this study. However, what is clear is that these equations utilise the return stroke model, $i\left(z,t\right)$. This expression for the lightning current along a path can be defined by different models as in [2, 4, 11]. All the models hold the form shown in *Equation 3.3* where $u(t)$ is the Heaviside function, $P(z')$ is the height-dependent current attenuation factor and $i(0,t)$ is the lightning channel base current which as the name suggests is the current as measured from the base of the object that is struck [2, 4, 12].

$$i(z',t) = u\left(t-\frac{z'}{v}\right)P\left(z'\right)i\left(0,t-\frac{z'}{v}\right) \tag{3.3}$$

In short, there are two steps of integration required to calculate induced currents on transmission lines [4, 11, 13].

1. Integrate some model of the lightning channel base current to obtain the EM fields.
2. Integrate the EM fields using the equations defined by Agrawal et al. to obtain the induced currents.

Referring back to *Figure 3.1*, the induced effects on a nearby transmission line can be calculated by modelling the lightning event as in *Figure 3.1(b)* and choosing an appropriate lightning channel base current. Clearly from the equations above, at least the second integral of this channel base current is required. Using an accurate lightning channel base current leads to very complex models that require long computer simulations because of numerical integration [4]. *Section 3.4* details two of the more common equations used as lightning channel base current models.

3.2.2 Frequency Components of Lightning Currents

Obtaining frequency components of a lightning strike are important for studies such as that done by Lee et al., where they are studying the effects of the lightning frequency components on human injury caused by a lightning strike [14]. In this study, Lee et al. utilise the double exponential function to obtain the frequency components of a lightning strike. The frequency components in the double exponential are found to be an order of magnitude different to those recommended by the standards [15].

The reason for such a study is that the sharp rise in the lightning current creates a broad-band current. Without using the Heidler function for such applications, it is difficult to standardise testing across the different fields of interest.

3.3 IEC 62305-1 - Lightning Protection Standard

The IEC 62305 is the lightning protection standard containing four parts. Where part one focuses on the general principles of lightning protection and parts two to four focus on more specific areas of lightning protection. IEC 62305-1 details all the relevant components of a lightning flash as well as all the terminology and standard values to utilise when designing systems such as LPSs.

Figure 3.2 shows an adaptation of Figure A.1 from the standard. This figure shows how the different stroke currents, such as the 0.25/100 and 10/350 are composed. T_1 is the rise time (number before the '/') and T_2 is the fall time (number after the '/').

Figures A.3 and A.4 in the standard show typical waveshapes expected from both downward and upward lightning flashes respectively. The three components identified in these images are the first short stroke, the subsequent short stroke and the long stroke. The first and subsequent short strokes are seen to be high current impulses with a sharp rise and a slower decay. The long stroke on the other hand is a lower current that is maintained for a comparatively long time.

Table A.1 in the standard shows the values that should be used in system designs. The values given here are the maximum change in current, the charge, the peak current, etc. With these values, systems can be designed to different LPLs. The values given in this table are based on the original studies done by Anderson and Eriksson and Berger et al. on lightning currents [16, 17]. The standard typically makes use of the upper end values to protect against more lightning events. For example, a system with a higher current rating will be protected against a lower current lightning strike.

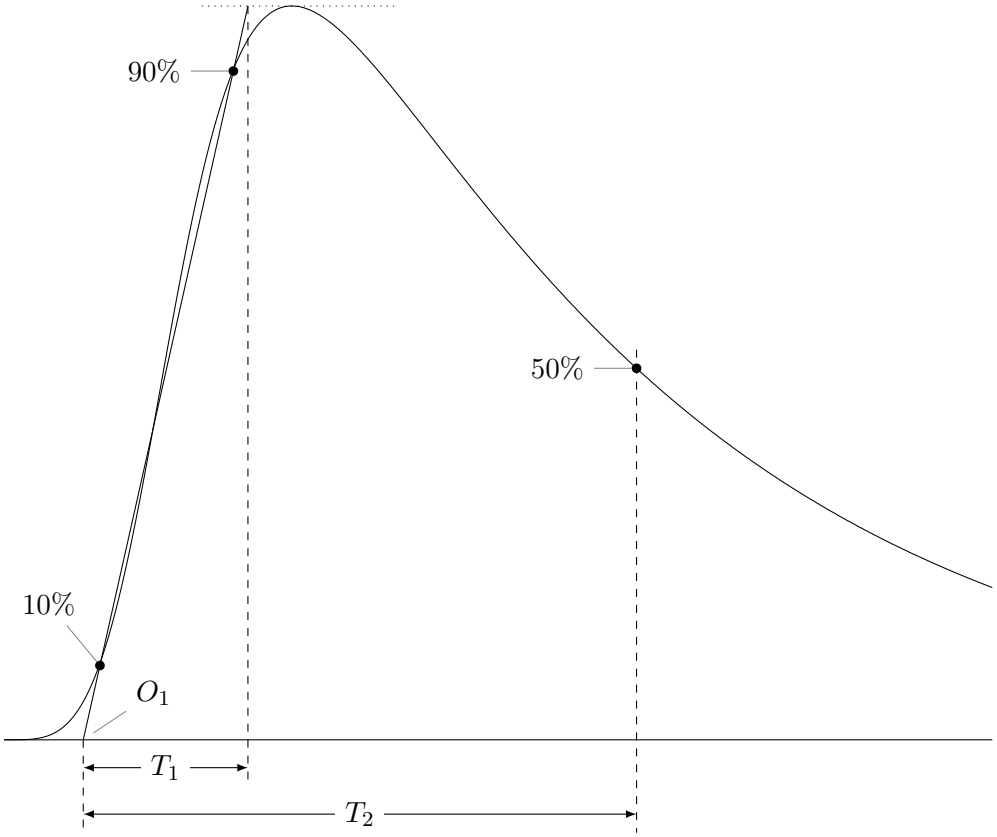


FIGURE 3.2: Definitions of short stroke parameters adapted from [1]

In order to simulate lightning currents in LPS design, the standard identifies a function that creates a waveshape with the characteristics outlined in Table A.1 of the standard. This function is the Heidler function with a specific configuration ($n = 10$) (see *Section 3.4.2*). This function can be used to create any lightning current waveshape with the two of interest in the standard being the 10/350 (first short stroke) and the 0.25/100 (subsequent short stroke). These two waveshapes are simulated using the parameters specified in Table B.1 in the standard for the different LPLs and stroke types [1].

3.4 Current Waveshape Models

The IEC lightning protection standard details the Heidler function with a specific configuration as the standardised waveshape for lightning current simulations. There are several lightning current models defined in the literature with the two most popular being the Heidler and the double exponential. There are also applications that use a combination of the two [11, 12, 18]. This section gives some background into these two equations and their properties.

3.4.1 The Double Exponential Model

The double exponential function is defined in *Equation 3.4.*

$$i_e(t) = \frac{I_o}{A}\left(e^{-\alpha t} - e^{-\beta t}\right) \tag{3.4}$$

Where:

I_0 = Peak current [A]

A = Peak current correction

α = Decay time constant [1/s]

β = Rise time constant [1/s]

The double exponential model is often used in place of the Heidler function because it can be integrated. However the waveshape produced by the double exponential equation is not physically realistic because the maximum current steepness occurs at time $t = 0$ [2, 3, 19, 20]. Moreover, this function does not allow for waveshapes that comply with Table A.1 in the IEC 62305-1 standard. For instance, a subsequent short stroke for LPL-I would have a maximum current steepness of about 545 kA/μs, which is far greater than the maximum value outlined in the standard of less than 200 kA/μs [21]. Another disadvantage to using this equation is that it is not easily adjustable, the parameters are not easily obtained for different waveshapes [12].

3.4.2 The Heidler Function

To avoid the disadvantages of the double exponential equation, the Heidler function is used. This can be seen in *Equation 3.5.*

$$i_h(t) = \frac{I_0}{\eta}\frac{\left(\frac{t}{\tau_1}\right)^{n_h}}{1+\left(\frac{t}{\tau_1}\right)^{n_h}}e^{-\frac{t}{\tau_2}} \tag{3.5}$$

Where:

I_0 = Peak current [A]

η = Peak current correction

τ_1 = Rise time constant [s]

τ_2 = Decay time constant [s]

n_h = Heidler steepness factor

This equation more realistically approximates a lightning return stroke and the peak current correction can be calculated using *Equation 3.6* [2, 12, 19, 20, 22].

$$\eta = e^{-\frac{\tau_1}{\tau_2}\left(\frac{n_h\tau_2}{\tau_1}\right)^{\frac{1}{n_h}}} \tag{3.6}$$

Equation 3.7 shows the first derivative of the Heidler function.

$$i'_h(t) = \frac{I_0}{\eta}\left(\frac{n_h t^{n_h-1}\tau_1^{n_h}}{\left(\tau_1^{n_h}+t^{n_h}\right)^2} - \frac{t^{n_h}}{\tau_2\left(\tau_1^{n_h}+t^{n_h}\right)}\right)e^{-\frac{t}{\tau_2}} \tag{3.7}$$

The IEC 62305-1 standard makes use of a specialised form of the Heidler function where $n_h = 10$. Using this form of the equation, there are values for the other parameters in the standard that can be used to simulate both first and subsequent short strokes [1, 21].

The disadvantage of the Heidler function is that there is no analytical integral and hence no analytical expression for the Heidler function in the frequency domain [2, 19]. This creates problems when performing analyses such as those mentioned in *Section 3.2* above.

3.5 Heidler Function Approximations

As there are is no analytical integral to the Heidler function, there are many researchers working towards an approximation that can be used in its place for applications such as those mentioned in *Section 3.2*. This section discusses a few of these approximations with the disadvantages associated with each one.

Feizhou and Shanghe developed a function that they call the *Pulse function* [2]. According to their study, this function produces a maximum error of 0.5% with the waveshapes they used. However, this function is a modified form of the double exponential function and it requires very complex methods to determine the parameters used in the equation.

Heidler and Cvetić approximate the Heidler function utilised in the IEC 62305-1 standard [3]. This approximation has an analytical integral but the equation is specific to the subsequent short stroke. There is no general form of this approximation and so this equation cannot be easily manipulated. Their study also details several other approximations to the Heidler function but all with other applications. They all have the disadvantage that they cannot be integrated analytically.

Delfino et al. conduct a study in which they develop a Prony series approximation to the Heidler function [20]. The mathematics required for this approximation is very complex limiting its use in engineering applications. Each scenario is different as there is no truly generalised form and the number of terms used affects the error associated with the approximation. This would be difficult to use for engineering applications.

Javor and Rancic develop a new approximation that they call the *New Channel Base Current (NCBC)* [12, 23]. This function contains some complicated mathematics and it is

a piecewise function which implies that there are discontinuities when taking the analytical derivative with step functions. The approximation also contains incomplete gamma functions which are defined as integrals and hence further complicate the mathematics [24]. There is no analytical Fourier transform to this approximation [25].

Vujević et al. define their version of the *exponential approximation* that is fixed for $n_h = 10$ [26, 27]. The mathematics presented in their study is extremely complicated and they introduce several new unknown parameters. The approximation is not as intuitive as the Heidler function. The frequency response presented is not as expected at higher frequencies; it does not roll off as it does in the standard.

All of the approximations above have one or more disadvantage or limitation. Overall the problems are that the mathematics are very complicated and it would be very difficult to simply substitute these equations in place of the Heidler function in the IEC 62305-1. The approximation in this dissertation provides an approximation, with an analytical integral, for use in engineering applications that does not have these limitations.

3.6 Conclusion

This chapter has given the background information relevant to this study. This includes all the terminology, equations, applications and a literature review.

The following chapter details the approximation that is developed in this study. The development of the function is detailed and all its properties are discussed in isolation.

Chapter 4

Heidler Function Approximation

This chapter deals with the development of the approximation. This is done by closely analysing the Heidler function and defining the limiting parts of the function. The development pathway of the approximation is detailed. The approximation is defined and its parameters are explained. The time domain properties (derivative and integral) and frequency domain properties (Fourier transform) are also discussed.

4.1 Overview

Knowledge of which parts of the Heidler function are preventing it from having an analytical integral allows for the development of an approximation. Once the Heidler function has been decomposed and understood, some insight into the solution can be gathered. As outlined in Chapter 2, the approximation function has certain criteria. Firstly, it must approximate the Heidler function in the time domain (within certain error limits). Secondly, it must have an analytical solution to its integral. Lastly, it must take the same form as the Heidler function so that the Heidler function and the approximation can be interchanged for different applications. With these criteria in mind the approximation function is developed.

4.2 Decomposing the Heidler Function

An example of the Heidler function can be seen in *Figure 4.1.* This function is defined by *Equation 3.5* in *Section 3.4.2.* The shorthand version of the equation can be seen in

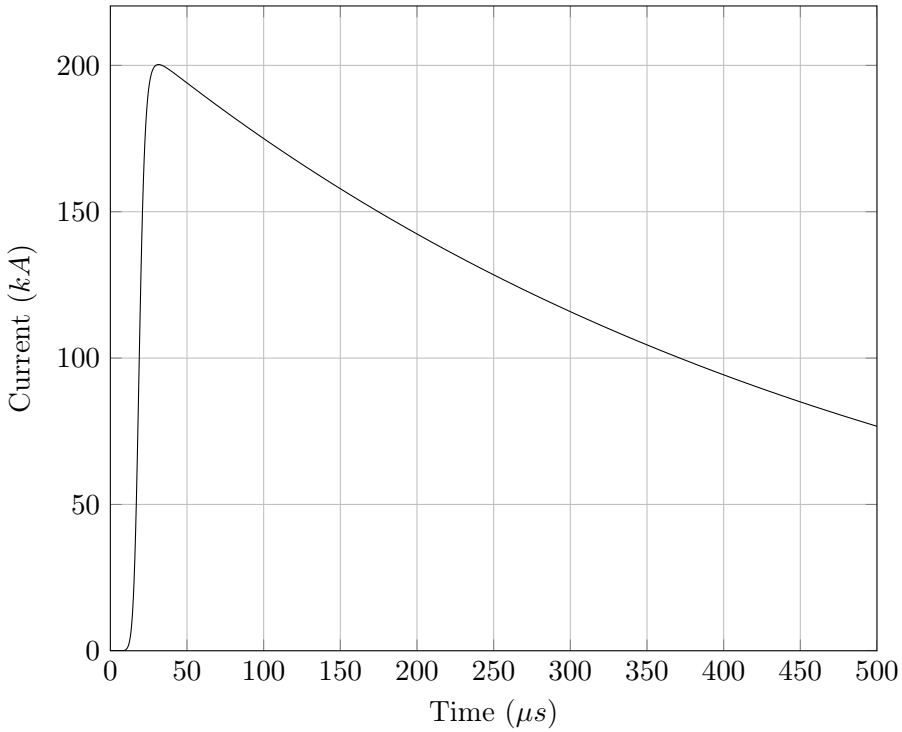


FIGURE 4.1: Graph depicting the Heidler function in the form of a 10/350 lightning waveform with a 200 kA peak.

Equation 4.1.

$$i_h(t) = \frac{I_0}{\eta} x_h(t)\, y(t) \tag{4.1}$$

Where

$$x_h(t) = \frac{\left(\frac{t}{\tau_1}\right)^{n_h}}{1 + \left(\frac{t}{\tau_1}\right)^{n_h}} \tag{4.2}$$

and

$$y(t) = e^{-\frac{t}{\tau_2}} \tag{4.3}$$

Equations 4.2 and *4.3* are the rise and fall components of the Heidler function respectively. The rise component cannot be analytically integrated preventing an analytical transform of the Heidler function into the frequency domain. These equations will be analysed in detail in *Sections 4.2.1* and *4.2.2* and an approximation that overcomes this limitation of the Heidler function is developed.

4.2.1 Heidler Rise Function

The rise time part of the Heidler function is defined by *Equation 4.2* and is plotted in *Figure 4.2*. This function ctakes the form of an S-curve. Clearly, this function can be easily modified to represent any lightning waveshape rise time. This can be achieved by

varying n_h (the steepness factor) and τ_1 (the rise time constant). Therefore this function meets the criteria that it can approximate any lightning waveform. However this function cannot be integrated and hence cannot be transformed into the frequency domain. In order to solve this limitation another S-curve must be developed that approximates this one and which can also be integrated.

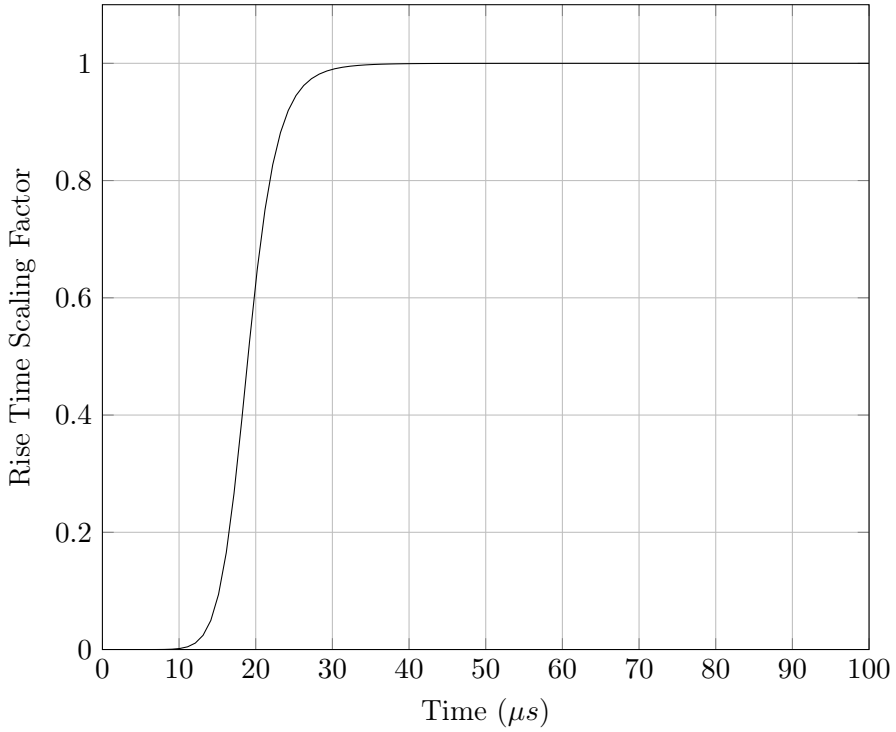


FIGURE 4.2: Graph depicting the rise function of the Heidler function (an S-curve).

There are numerous forms of the S-curve such as those given in *Equation 4.4a* to *Equation 4.4f*.

$$f(x) = \operatorname{erf}\left(\frac{\sqrt{\pi}}{2}x\right) \tag{4.4a}$$

$$f(x) = \frac{x}{\sqrt{1+x^2}} \tag{4.4b}$$

$$f(x) = \tanh(x) \tag{4.4c}$$

$$f(x) = \frac{2}{\pi}\arctan\left(\frac{\pi}{2}x\right) \tag{4.4d}$$

$$f(x) = \frac{2}{\pi}\operatorname{gd}\left(\frac{\pi}{2}x\right) \tag{4.4e}$$

$$f(x) = \frac{x}{1+|x|} \tag{4.4f}$$

These equations do not allow for an easy manipulation of parameters to tailor the waveshape to a specific rise time and steepness. Many of these functions can also not be

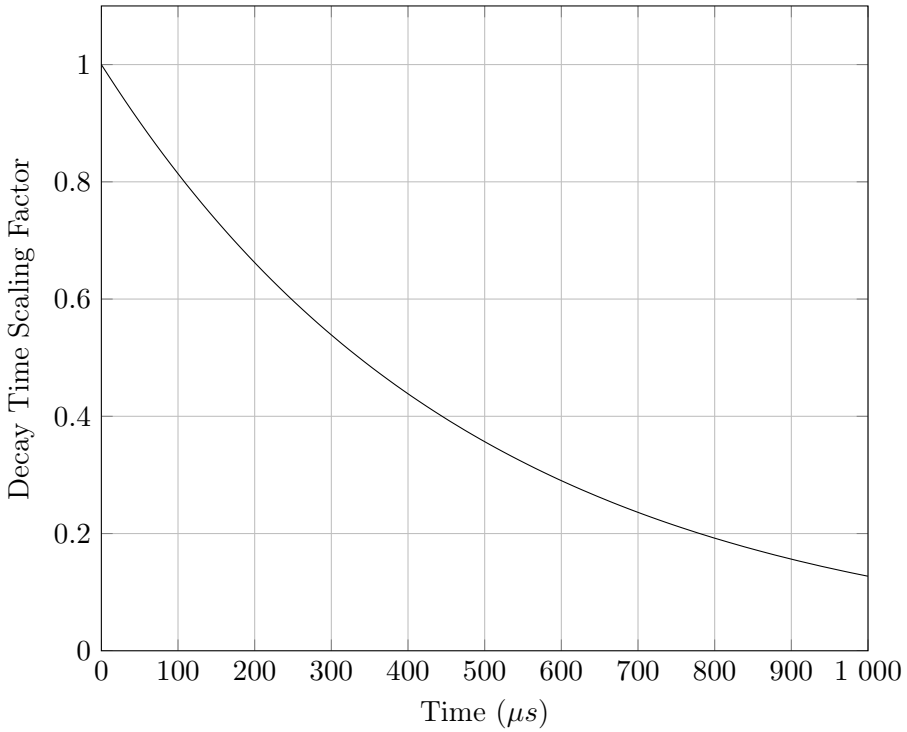


FIGURE 4.3: Graph depicting the decay function of the Heidler function (exponential decay function).

integrated which would not solve the limitation of the Heidler function. Therefore an alternative is required that can easily be modified.

4.2.2 Heidler Fall Function

The part of the Heidler function that controls the decay time and shape is in *Equation 4.3* and a graph of this is plotted in *Figure 4.3*. This function clearly meets all the criteria outlined above: it can easily be altered to change the decay time and it can be trivially integrated (and hence transformed into the frequency domain). This function is just a complex shift of the signal in the frequency domain because of the rule of Laplace transforms shown in *Equation 4.5* [28, 29].

$$\mathcal{L}\left\{e^{-at} f(t)\right\} = F(s+a) \tag{4.5}$$

Therefore there is no need to redefine the decay part of the equation in any way and the approximation function can still be defined as *Equation 4.6*.

$$i_a(t) = \frac{I_0}{\eta} x_a(t)\, y(t) \tag{4.6}$$

Where I_0, η and $y(t)$ as per the Heidler function (*Equation 3.5*) and:

$x_a(t)$ = The rise function of the approximation

The next section details the development of the approximation function.

4.3 Developing an Approximation to the Heidler Function

The development of this approximation is different to the approaches taken for the approximations in the literature (see *Chapter 3*). The only part of the Heidler function that is approximated is the rise function ($x_h(t)$) and the approximation is developed in the Laplace domain ensuring that the time domain equation can be integrated analytically [30].

This implies that the rise equation that is developed must be transformed into the time domain. The decay equation and peak current can be used with this to obtain the overall approximation equation.

The step response of an n-th order, real and negative pole creates an S-curve in the time domain. *Equation 4.7* shows the start of the approximation in the Laplace domain, the step response of an n-th order pole. See *Appendix A* for the full step-by-step process in getting from this point to the final approximation.

$$X_a(s) = \frac{1}{s\left(\frac{s}{\omega_0}+1\right)^{n_a}} \tag{4.7}$$

Where:

ω_0 = Rise time constant [rad/s]

n_a = Approximation steepness factor

Taking the inverse Laplace transform of this equation, the rise function of the approximation is found as shown in *Equation 4.8*.

$$x_a(t) = 1 - e^{-\omega_0 t}\left(\sum_{i=0}^{n_a}\frac{\omega_0^i t^i}{i!}\right) \tag{4.8}$$

The constants in this equation can be varied to obtain different steepness factors and rise times (see *Sections 4.4.1* and *4.4.2* respectively). This function is plotted in *Figure 4.4*. This is clearly comparable to *Figure 4.2* which shows the rise time function of the Heidler function.

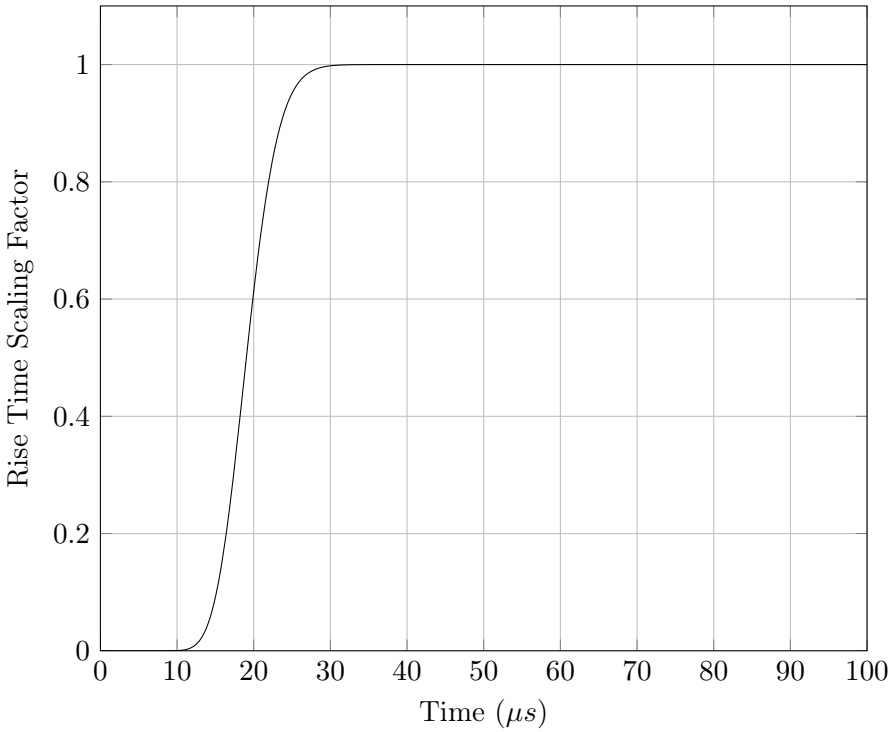


FIGURE 4.4: Graph depicting the rise function of the approximation function (an S-curve).

By substituting the approximated rise function back into the Heidler function shown in *Equation 4.1*, the overall approximation can be obtained. The next section details the approximation function, its properties and its frequency domain representation.

4.4 Function Definition and Properties

This approximation to the Heidler function has the advantage that it has an analytical integral and hence an analytical solution in the frequency domain. Moreover it can still be tailored to any waveshape, meaning that the steepness of the graph, the rise time, the fall time and the peak current can all be modified. This allows for analyses using 10/350, 0.25/100 and any other lightning waveshapes required.

The approximation function is defined in *Equation 4.9*.

$$i_a(t) = \frac{I_0}{\eta}\left(1 - e^{-\omega_0 t}\left(\sum_{i=0}^{n_a}\frac{\omega_0^i t^i}{i!}\right)\right)e^{-t/\tau_2} \tag{4.9}$$

Where:

I_0 = Peak current [A]

η = Correction factor of peak current

ω_0 = Rise time constant [rad/s]

τ_2 = Fall time constant [s]

n_a = Approximation steepness factor

Modifying these properties gives the desired lightning current waveform. An example plot of this function can be seen in *Figure 4.5*.

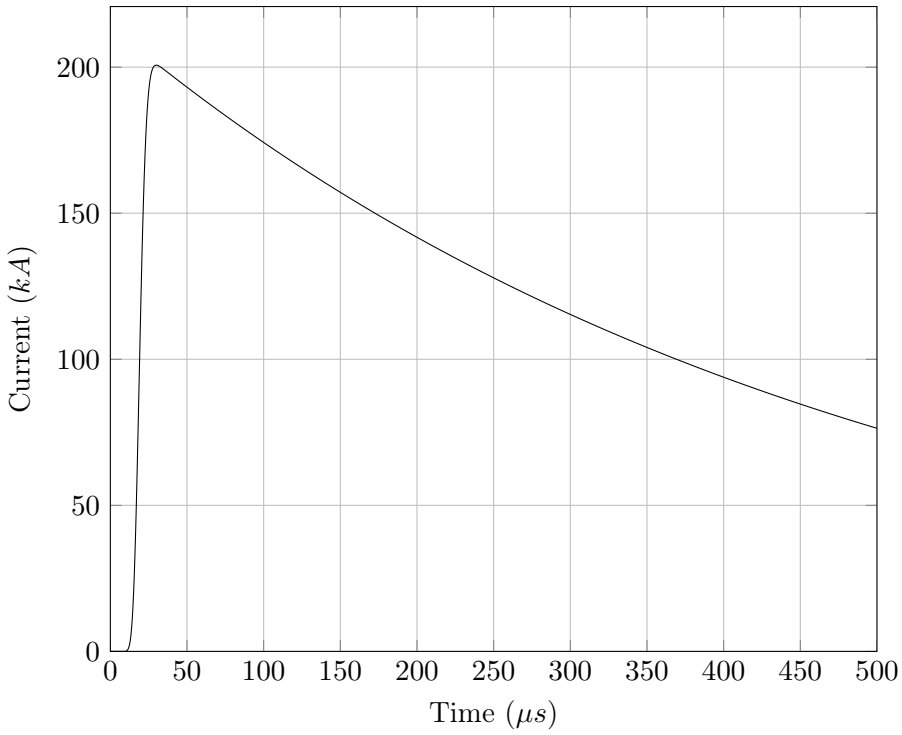


FIGURE 4.5: Graph of an example Heidler function approximation lightning current waveshape in the form of a 10/350 with a 200 kA peak current.

As the approximation was designed as a modification of the Heidler function, it still takes the same form as in *Equation 4.1* with $x_h(t)$ replaced with $x_a(t)$. The difference is that $x_h(t)$ cannot be integrated but $x_a(t)$ can be integrated and hence transformed into the frequency domain. The following subsections show how the steepness factor, rise time constant and fall time constant affect the shape and properties of the approximation function.

4.4.1 Steepness Factor

The steepness factor of the approximation, n_a, changes the shape of the approximation function. *Figure 4.6* shows several plots of the approximation function with different

steepness factors but constant rise time constant (ω_0), fall time constant (τ_2), peak current (I_0) and correction factor (η). These values are tabulated in *Table 4.1* where the values of I_0, η and τ_2 are obtained from the IEC 62305-1 standard and ω_0 is determined empirically for a 10/350 waveshape.

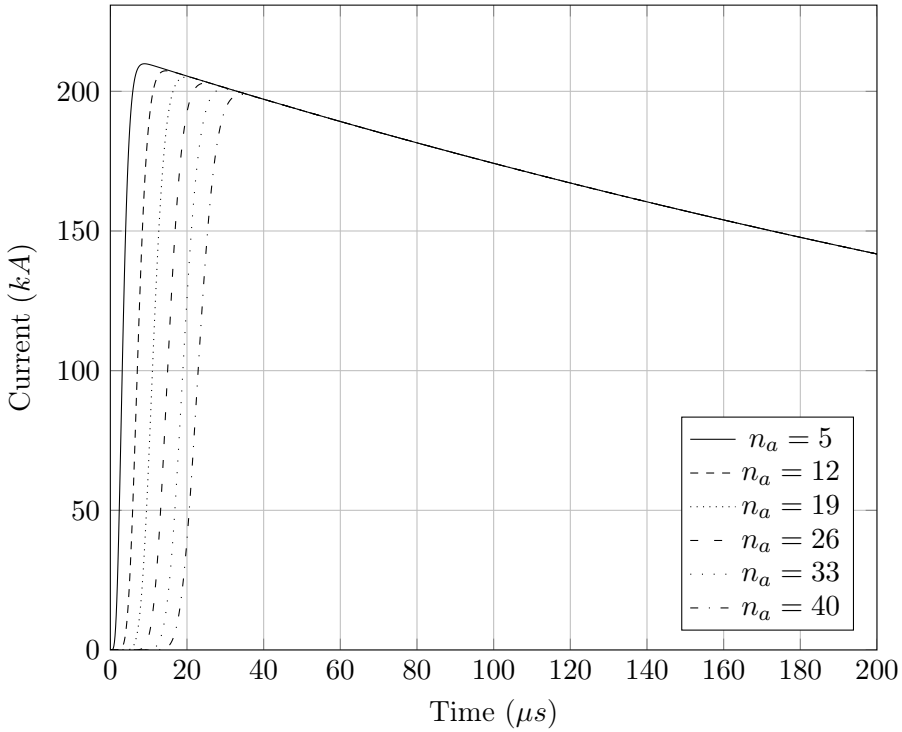


FIGURE 4.6: Graph showing the effect of changing the steepness factor (n_a) in the approximation function while keeping all the other variables constant.

TABLE 4.1: Constant values used in *Equation 4.9* to obtain the graphs plotted in *Figure 4.6*

Variable	**Value**
I_0	200 kA
η	0.93
ω_0	1 768 000 rad/s
τ_2	485 μs

As expected from *Equations 4.8* and *4.9*, the steepness factor only affects the rise function ($x_a(t)$) of the entire function. From the figure, it is clear that an increased steepness factor decreases the steepness of the rise time. The initial knee in the curve (upward bend) is delayed by a higher value of n_a and hence the maximum instantaneous change in current occurs later in time. The figure also shows that the rise time of the waveshape changes with a change in n_a but this is not the defining change.

Table 4.2 shows the peak current and rise time errors as the steepness factor changes. These errors are calculated as a percentage of a 10/350, 200 kA waveshape. Clearly the

error in rise time is more pronounced than the peak current error. This table gives an indication to the sensitivity of the function with a change in the steepeness factor (n_a).

TABLE 4.2: Variation of rise time and peak current of the approximation with a change in the steepness factor (n_a) as a percentage of a 200 kA 10/350 waveshape.

n_a	**Peak Current Error (%)**	**Rise Time Error (%)**
5	4.93	57.40
12	3.67	36.64
19	2.54	21.30
26	1.46	9.67
33	0.43	1.91
40	0.57	12.17

4.4.2 Rise Time Constant

The rise time constant, ω_0, is used primarily to change the rise time (the number before the '/') of the waveshape. *Figure 4.7* shows the effect of changing the rise time constant in the approximation while keeping the rest of the parameters constant. The constant values used in this plot are tabulated in *Table 4.3* where once again, I_0, η and τ_2 are obtained from the IEC 62305-1 standard and n_a is determined empirically for a 10/350 waveshape.

TABLE 4.3: Constant values used in *Equation 4.9* to obtain the graphs plotted in *Figure 4.7*

Variable	**Value**
I_0	200 kA
η	0.93
n_a	33
τ_2	485 μs

This plot clearly shows how the rise time changes with a change in the rise time constant. A greater rise time constant results in a faster rise time. The change in ω_0 also has an effect on the steepness of the graph but the defining feature is the change in rise time.

Table 4.4 shows the peak current and rise time errors as the rise time constant changes. Again, these errors are calculated as a percentage of a 10/350, 200 kA waveshape. As with the steepness factor, the error in rise time is more pronounced than the error in peak current. This table gives an indication to the sensitivity of the function with a change in the rise time constant (ω_0).

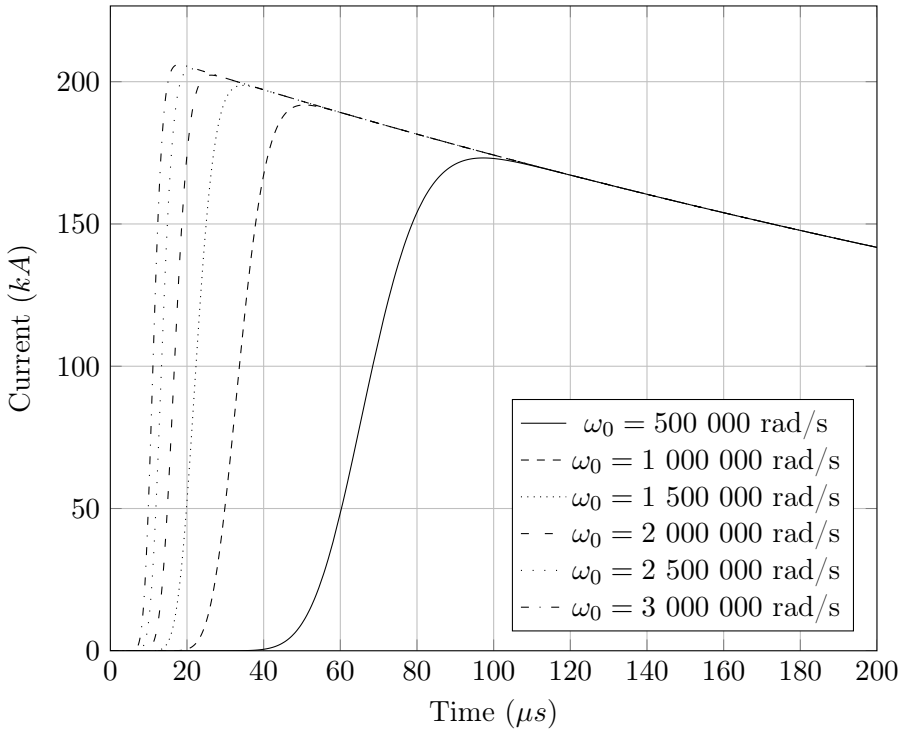


FIGURE 4.7: Graph showing the effect of changing the rise time constant (ω_0) in the approximation function while keeping all the other variables constant.

TABLE 4.4: Variation of rise time and peak current of the approximation with a change in the rise time constant (ω_0) as a percentage of a 200 kA 10/350 waveshape.

ω_0 **(rad/s)**	**Peak Current Error (%)**	**Rise Time Error (%)**
500000	13.40	243.67
1000000	4.09	77.36
1500000	0.65	20.31
2000000	1.15	9.12
2500000	2.25	27.29
3000000	3.01	38.91

4.4.3 Fall Time Constant

The fall time constant, τ_2, changes the decay time (the number after the '/') of the waveshape. *Figure 4.8* shows the effect of changing the fall time constant in the approximation function with the other parameters all fixed. These static values are seen in *Table 4.5* where once again, I_0 and η are obtained from the IEC 62305-1 standard and ω_0 and n_a are determined empirically for a 10/350 waveshape.

Several observations are made in this graph, namely:

1. This is the same effect as that seen in the Heidler function, as expected.

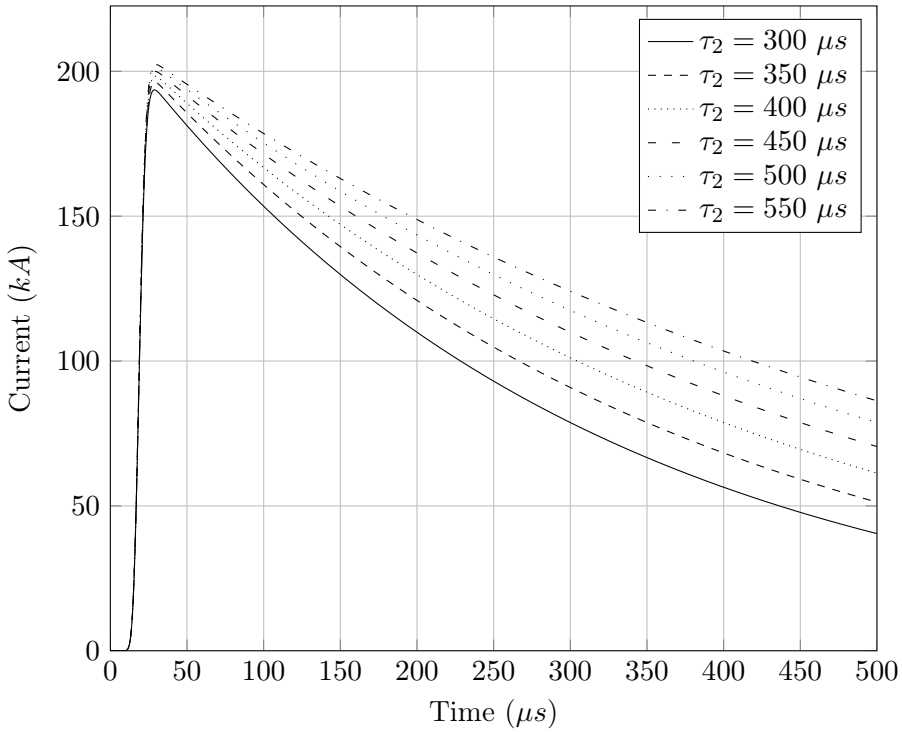


FIGURE 4.8: Graph showing the effect of changing the fall time constant (τ_2) in the approximation function while keeping all the other variables constant.

TABLE 4.5: Constant values used in *Equation 4.9* to obtain the graphs in *Figure 4.8*

Variable	**Value**
I_0	200 kA
η	0.93
n_a	33
ω_0	1 768 000 rad/s

2. As with the Heidler function, the decay time (the time to 50% of the peak current) is not the same as the decay time constant (τ_2).

3. The peak current varies slightly with the change in fall time constant as expected from *Equation 3.6*.

Table 4.6 shows the peak current and rise time errors as the fall time constant changes. Again, these errors are calculated as a percentage of a 10/350, 200 kA waveshape. This table is different to those of the steepness factor and rise time constant (*Tables 4.2* and *4.4*) because the fall time constant has a negligible effect on the rise part of the waveshape. This table gives an indication to the sensitivity of the function with a change in the fall time constant (τ_2).

TABLE 4.6: Variation of rise time and peak current of the approximation with a change in the fall time constant (τ_2) as a percentage of a 200 kA 10/350 waveshape.

τ_2 (μs)	**Peak Current Error (%)**	**Rise Time Error (%)**
300	3.22	0.35
350	1.88	1.51
400	0.85	1.68
450	0.04	1.83
500	0.61	1.95
550	1.16	2.05

4.5 Time Domain Properties

This section shows the time domain properties of the approximation namely, the time derivative and the integral. Unlike the Heidler function, the approximation has an analytical integral.

4.5.1 Derivative

Equation 4.10 shows the analytical derivative of the approximation. This shows the rate of change of the current in the lightning stroke current model.

$$i'_a(t) = \frac{I_0}{\eta}\left[e^{-\omega_0 t}\left(\frac{\omega_0^{n_a+1}t^{n_a}}{n_a!}\right) - \frac{1}{\tau_2}\left(1 - e^{-\omega_0 t}\left(\sum_{i=0}^{n_a}\frac{\omega_0^i t^i}{i!}\right)\right)\right]e^{-\frac{t}{\tau_2}} \tag{4.10}$$

A graph of the above function with the same parameters as those utilised in creating the graph in *Figure 4.5*, can be seen in *Figure 4.9*. As is expected, the greatest rate of change of current occurs during the rise of the graph and the negative rate of change is comparatively small.

4.5.2 Integral

One of the primary reasons for developing an approximation to the Heidler function is to have the ability to integrate such a function. Obtaining the integral of the approximation is trivial and can be seen in *Equation 4.11* where C is some arbitrary constant of integration because it is an indefinite integral.

$$\int i_a(t)\,dt = \frac{I_0\tau_2 e^{-t\left(\frac{1}{\tau_2}+\omega_0\right)}}{\eta}\left(-e^{t\omega_0} + \sum_{i=0}^{n_a}\frac{\omega_0^i}{i!}\sum_{j=0}^{i}\frac{i!\,\tau_2^j t^{i-j}}{(i-j)!\,(\tau_2\omega_0+1)^{j+1}}\right) + C \tag{4.11}$$

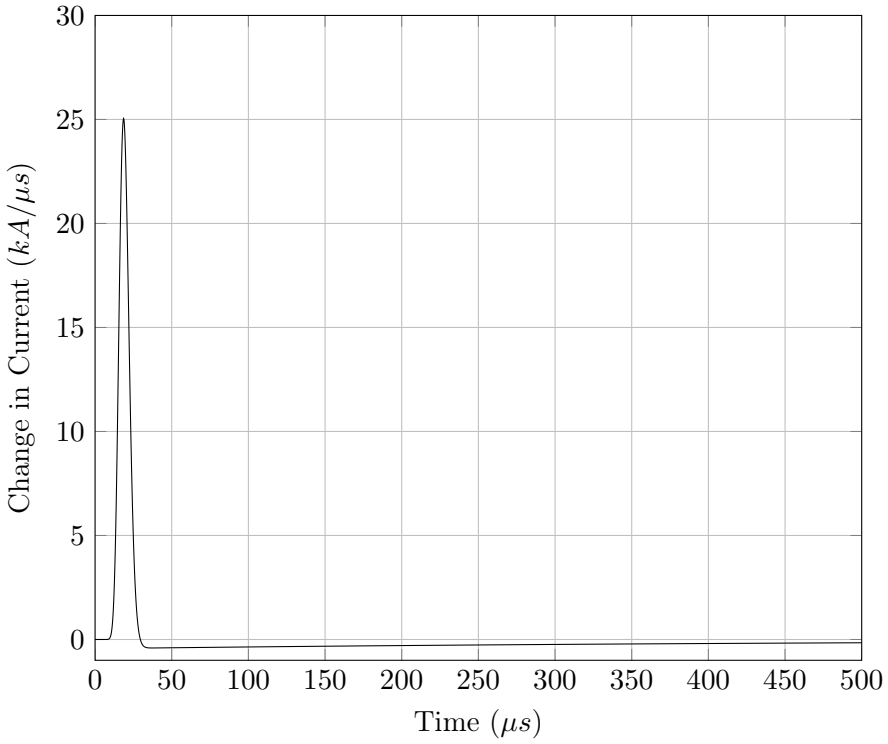


FIGURE 4.9: Graph showing the derivative of the approximation function shown in *Figure 4.5*.

4.6 Frequency Domain Properties

Another reason for using an approximation to the Heidler function is to obtain a Fourier transform and hence a current density or frequency response. The approximation shown in *Equation 4.9* makes this process even more trivial. Rather than using the fact that the approximation can be integrated (see *Section 4.5.2*), the approximation is developed in the Laplace domain. Hence the Fourier transform is found by using the complex shifting property of Laplace (see *Equation 4.5*) and replacing s with $j\omega$. The result of this can be seen in *Equation 4.12*.

$$I_a\left(j\omega\right) = \frac{I_0}{\eta}\frac{1}{j\omega + \frac{1}{\tau_2}}\frac{1}{\left(\frac{j\omega + \frac{1}{\tau_2}}{\omega_0} + 1\right)^{n_a}} \tag{4.12}$$

By using dimensional analysis, it can be seen that in *Equation 4.12*, $I_a(j\omega)$ has the units of A/Hz. This implies a current density across the angular frequency spectrum. In order to obtain current density as a function of frequency, ω should be replaced by $2\pi f$ as seen in *Equation 4.13*.

$$I_a\left(jf\right) = \frac{I_0}{\eta}\frac{1}{j2\pi f + \frac{1}{\tau_2}}\frac{1}{\left(\frac{j2\pi f + \frac{1}{\tau_2}}{\omega_0} + 1\right)^{n_a}} \tag{4.13}$$

Equations 4.12 and *4.13* are complex functions and the modulus is required to plot the current density of the approximation. The modulus is shown in *Equation 4.14* and a plot of this equation, based on the waveshape shown in *Figure 4.5*, can be seen in *Figure 4.10*.

$$\begin{aligned} |I_a(jf)| &= \left| \frac{I_0}{\eta} \frac{1}{j2\pi f + \frac{1}{\tau_2}} \frac{1}{\left(\frac{j2\pi f + \frac{1}{\tau_2}}{\omega_0} + 1\right)^{n_a}} \right| \\ &= \frac{I_0}{\eta} \frac{1}{\sqrt{\frac{1}{\tau_2^2} + 4\pi^2 f^2}} \frac{1}{\left(\sqrt{\left(1 + \frac{1}{\omega_0 \tau_2}\right)^2 + \frac{4\pi^2 f^2}{\omega_0^2}}\right)^{n_a}} \end{aligned} \tag{4.14}$$

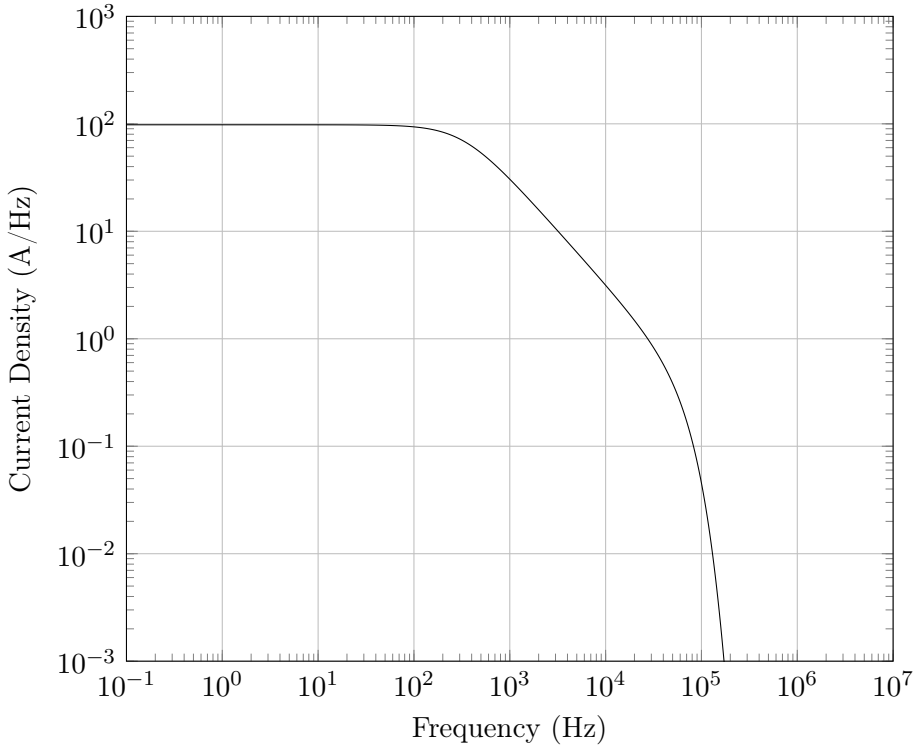


FIGURE 4.10: Amplitude density of the approximation model produced from the waveshape plotted in *Figure 4.5*.

4.7 Conclusion

This chapter has decomposed the Heidler function into its components and found an approximation to the rise time function that can be used in the general form of the equation. The approximation has been detailed with all its parameters. Its time domain and frequency domain properties have been discussed. The following chapter explains how results are obtained and shows the simulated results.

Chapter 5

Results: A Comparison to the Heidler Function

This chapter shows the results obtained by simulating the approximation and comparing the simulations to those of the Heidler function. In order for the results to be understood, the experimental methodology is first defined which explains how the simulations are carried out and how the comparisons are made. Both the first short stroke and the subsequent short stroke (10/350 and 0.25/100 respectively) are analysed. In the analyses, the functions and their derivatives are compared to the Heidler function and the current densities of the approximation are plotted.

5.1 Overview

As mentioned in *Chapter 2*, the results obtained in this study are simulated. The simulations used in this study are those of the short lightning current waveshapes detailed in the IEC 62305-1 standard [1]. These are the initial and subsequent short strokes (10/350 and 0.25/100 respectively). This chapter details the experimental methodology and compares the waveshapes obtained using the Heidler function (*Equation 3.5*) with those obtained using the approximation (*Equation 4.9*).

5.2 Experimental Methodology

The requirement in this study is to determine the accuracy of the approximation to the Heidler function. This is achieved by running mathematical simulations using mathematical modelling software such as MATLAB® [31], Mathematica® [32], Maxima [33], etc. In order to determine a level of accuracy, the values used in the IEC 62305-1 are used as a control. The parameters used in creating the Heidler function are detailed in Table B.1 of the IEC 62305-1 standard. These values are for the 10/350 and the 0.25/100 waveshapes (first and subsequent short strokes respectively).

Initial values are estimated for the parameters of the approximation from the Heidler function parameters mentioned above. These values are then empirically optimized in order to minimize the error between the approximation and the Heidler waveshapes. These tabulated and calculated parameters are utilised in *Equations 3.5* and *4.9* respectively to evaluate the accuracy of the approximation. An n_a of 33 is found to be appropriate for the waveshapes defined in the standard which have an n_h of 10 (see *Chapter 6* for more).

There are various peak current values for the different LPLs defined in Table B.1 in the standard [1]. However, as the peak current is only determined by I_0 (peak current) and η (peak current correction), the peak current values have no effect on the waveshapes defined in *Equations 3.5* and *4.9* or their respective errors.

The evaluation includes three simulations per waveshape. These are the current waveshape, the change in current (first derivative) and the current density (Fourier transform).

The current waveshapes of the Heidler function and the approximation are plotted with the required parameters. The absolute value of the difference between the two functions is determined and the maximum error is defined from this as a percentage of the Heidler function. The first derivative is evaluated in very much the same manner as the current waveshape.

The current density is evaluated by using the parameters calculated for the approximation in *Equation 4.13*. This is then plotted on log-log axes. As there is no analytical Fourier transform of the Heidler function, this is purely an indication and no quantification of error can be obtained from this.

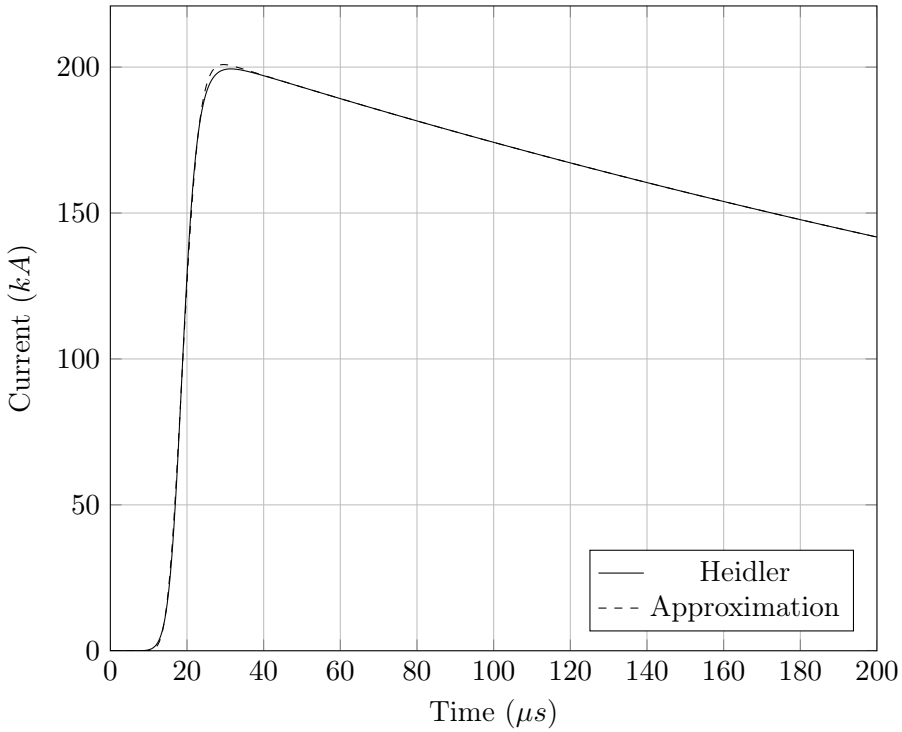


FIGURE 5.1: Graph of the first short stroke (10/350) current model using both the Heidler function and the approximation. The time scale is up to 200 μs and the amplitude is as high as 210 kA.

5.3 First Short Stroke (10/350)

The first short stroke as defined by the IEC 62305-1 has a front time of 10 μs and a decay time of 350 μs (see *Section 3.3*) [1]. A graph depicting both the Heidler function (solid line) and the approximation (dashed line) waveshapes can be seen in *Figure 5.1*. The values used in both of the equations to create the waveshapes seen in *Figure 5.1* are shown in *Table 5.1*.

TABLE 5.1: Parameters used in *Equations 3.5* and *4.9* to plot the waveshapes shown in *Figure 5.1*.

Parameter	**Heidler**	**Approximation**
I_0 [kA]	200	200
η	0.93	0.93
n_a	-	33
n_h	10	-
ω_0 [rad/s]	-	1 768 211
τ_1 [μs]	19	-
τ_2 [μs]	485	485

It is clear from the figure that the approximation closely follows the waveshape produced by the Heidler function. The error is quantified by determining the error as a function

of time as seen in *Equation 5.1*. The maximum error is found by equating the first time derivative of the error function to zero as in *Equation 5.2* and solving for t. This time is substituted back into the error function to obtain the maximum error in kA. This value is found as a percentage of the peak value of the Heidler function.

$$e(t) = |i_a(t) - i_h(t)| \tag{5.1}$$

$$e'(t) = 0 \tag{5.2}$$

Where:

$e(t)$ = Error function [A]

$e'(t)$ = Derivative of error function [A/s]

In the case of the 10/350 waveshape, with the parameters defined in *Table 5.1*, the maximum error is defined as 1.38%. This error is seen to occur during the rise part of the waveshape which is expected because the decay functions are identical.

The next comparison made is between the first derivatives of both the Heidler function and the approximation (*Equations 3.7* and *4.10* respectively). This shows the difference in the instantaneous change in current of the two waveshapes. The same parameters are used, i.e. those in *Table 5.1*. The graph showing both of these waveshapes can be seen in *Figure 5.2*.

The error is more pronounced in the derivative. Using the same method as above to obtain the maximum error as a percentage of the Heidler function maximum, the maximum error is calculated to be 7.91% (as before, the error is seen during the rise part of the waveshape).

The maximum dI/dt occurs during the rise time of the function. Another characteristic of the plot is that the exponential decay is much longer than the rise. This causes the negative component of the derivative to be much smaller but longer than the rise time component.

In both *Figures 5.1* and *5.2*, the time scale goes up to 200 μs. This is because the tails of the two waveshapes are the same. Therefore the resolution needs to be shown on the rise time of the waveshapes. The amplitudes shown in the two graphs are large enough to show the maximum values (200 kA in *Figure 5.1* and 27.5 kA/μs in *Figure 5.2*).

For completeness, the current density of the approximated first short stroke is plotted in *Figure 5.3*. This is produced using *Equation 4.13* and the parameters in *Table 5.1*. A current density is plotted because this is what is shown in Figure B.5 in the IEC 62305-1 standard.

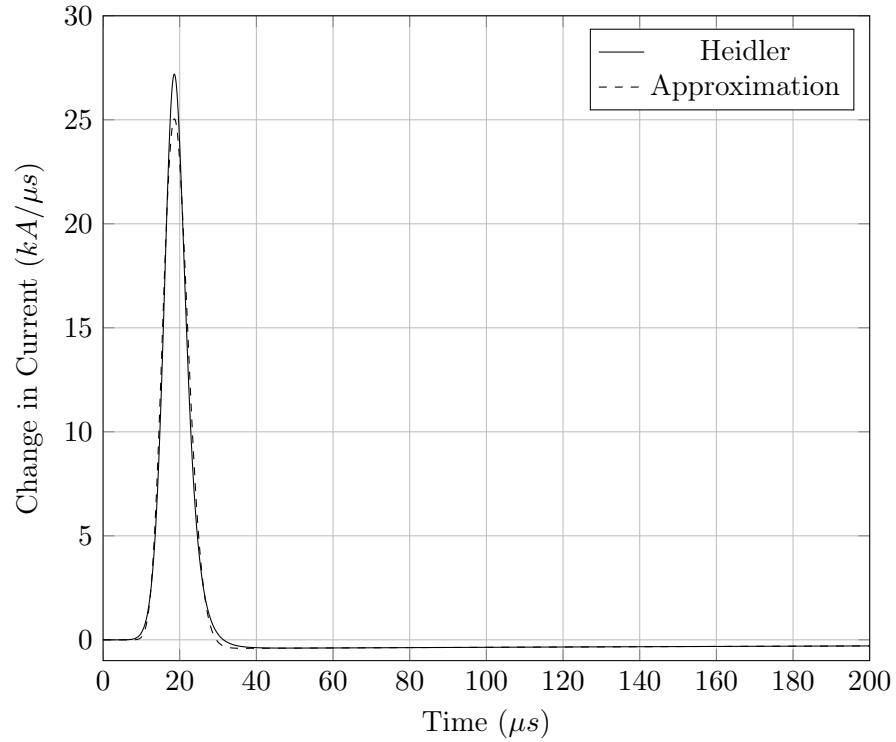


FIGURE 5.2: Graph of the first time derivative of the first short stroke (10/350) current model using both the Heidler function and the approximation. The time scale is up to 200 μs and the amplitude is as high as 30 kA/μs.

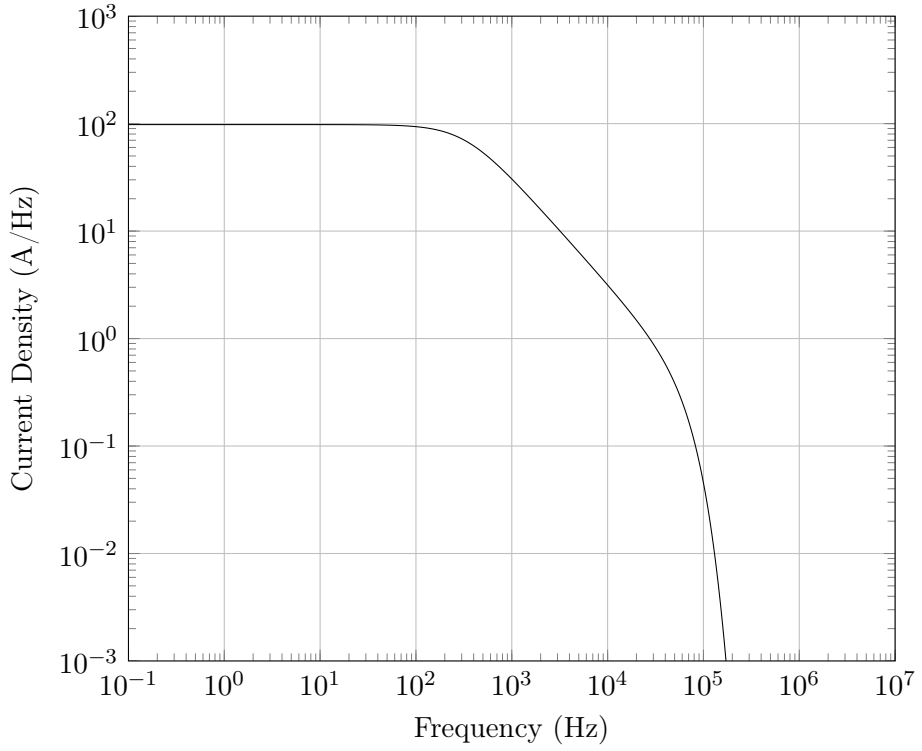


FIGURE 5.3: Current density of the approximation model produced from the waveshape plotted in *Figure 5.1*.

It is difficult to calculate an error in the case of the current density as there is no analytical solution to the integral and hence the Fourier transform of the Heidler function. Therefore any representation of this would be based on numerical methods with inherent errors.

5.4 Subsequent Short Stroke (0.25/100)

As stated in *Chapter 2*, the purpose of this study is to find an appropriate approximation to the Heidler function that can be used as a substitute when designing systems using the guidelines of the IEC 62305-1 standard. Therefore both the waveforms prescribed by the standard need to be analysed. Because of this, this section is similar to the last. However slightly different conclusions can be drawn from the two different waveshapes.

According to the standard, the subsequent short stroke has a front duration of 0.25 μs and a decay time of 100 μs [1]. This implies a much sharper rise time than that of the first short stroke. Again, the three metrics shown here are the actual waveshape, the first time derivative and the current density.

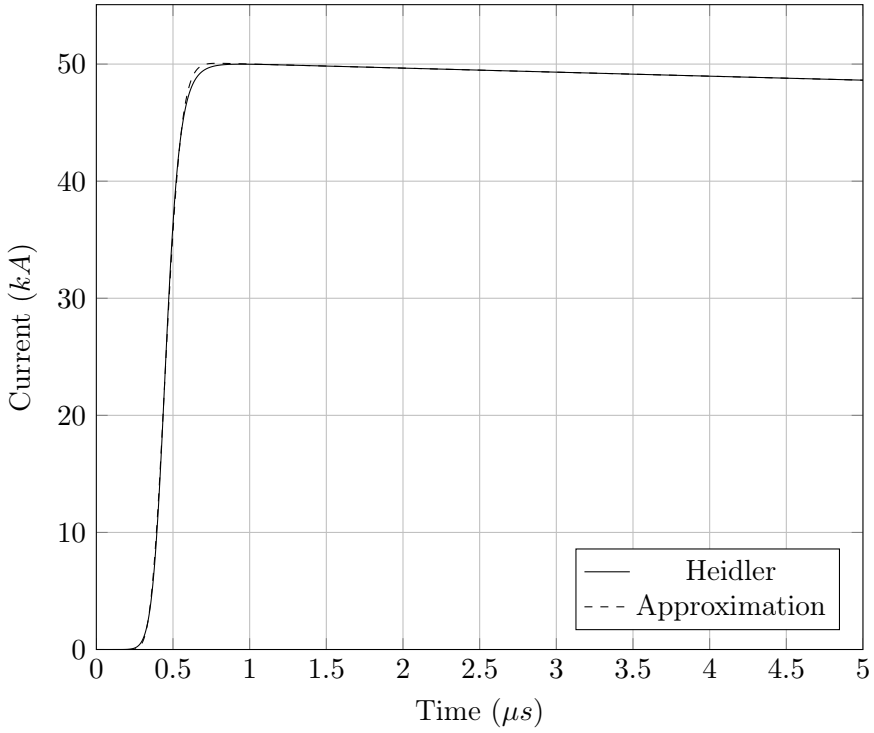


FIGURE 5.4: Graph of a subsequent short stroke (0.25/100) current model using both the Heidler function and the approximation. The time scale is up to 5 μs and the amplitude is as high as 52 kA.

A graph depicting both the Heidler function (solid line) and the approximation (dashed line) waveshapes can be seen in *Figure 5.4*. The values used in both of the equations to create the waveshapes seen in *Figure 5.4* are shown in *Table 5.2*.

TABLE 5.2: Parameters used in *Equations 3.5* and *4.9* to plot the waveshapes shown in *Figure 5.4*.

Parameter	**Heidler**	**Approximation**
I_0 [kA]	50	50
η	0.993	0.993
n_a	-	33
n_h	10	-
ω_0 [rad/s]	-	74 000 000
τ_1 [μs]	0.454	-
τ_2 [μs]	143	143

With the method outlined above, the maximum error is calculated to be 1.36% (as before, the error is seen during the rise part of the waveshape). The decay time is so much greater than the front duration (400×), that there is almost no decay in the graph shown. This is so that the variation in the rise part of the function can be seen.

The first time derivative of both the Heidler function (solid line) and the approximation (dashed line) are shown in *Figure 5.5*. Again the error in the first time derivative is

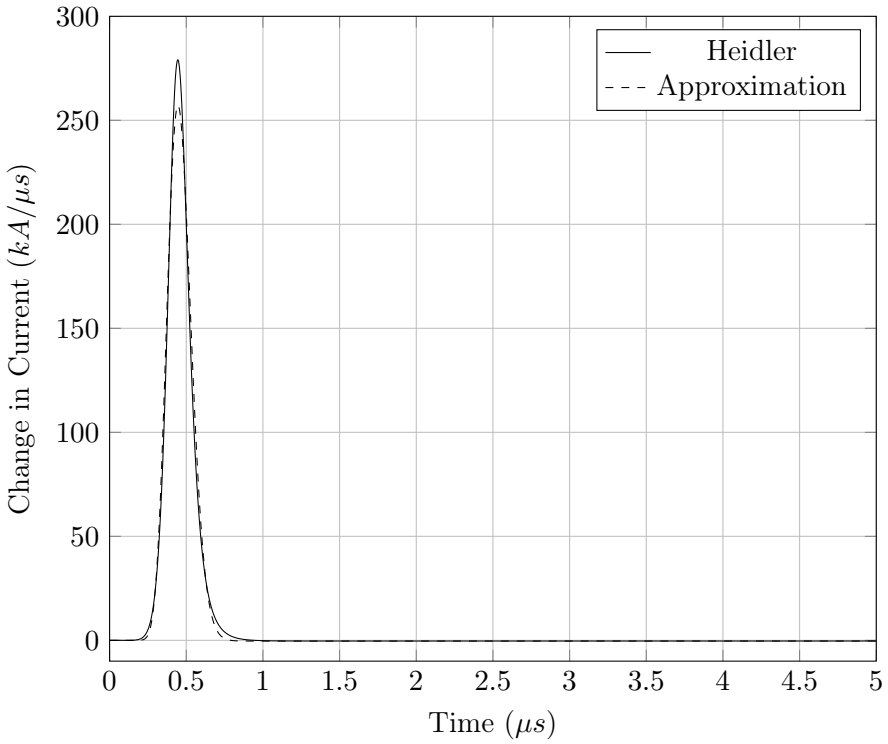


FIGURE 5.5: Graph of the first time derivative of a subsequent short stroke current model using both the Heidler function and the approximation. The time scale is up to 5 μs and the amplitude is as high as 300 kA/μs.

more pronounced than in the actual waveshape and this error is calculated to be 7.86% (as before, the error is seen during the rise part of the waveshape). The decay time is so large in comparison to the rise time, that the negative dI/dt is negligible and in most engineering applications can be assumed to be zero. The maximum change in current is ten times greater than that of the first return stroke.

Once again, the current density of the approximated subsequent short stroke can be seen in *Figure 5.6*. This is produced using *Equation 4.13* and the parameters in *Table 5.2*. As expected, there are higher frequency components in the subsequent short stroke than in the first short stroke. However, the amplitude is lower.

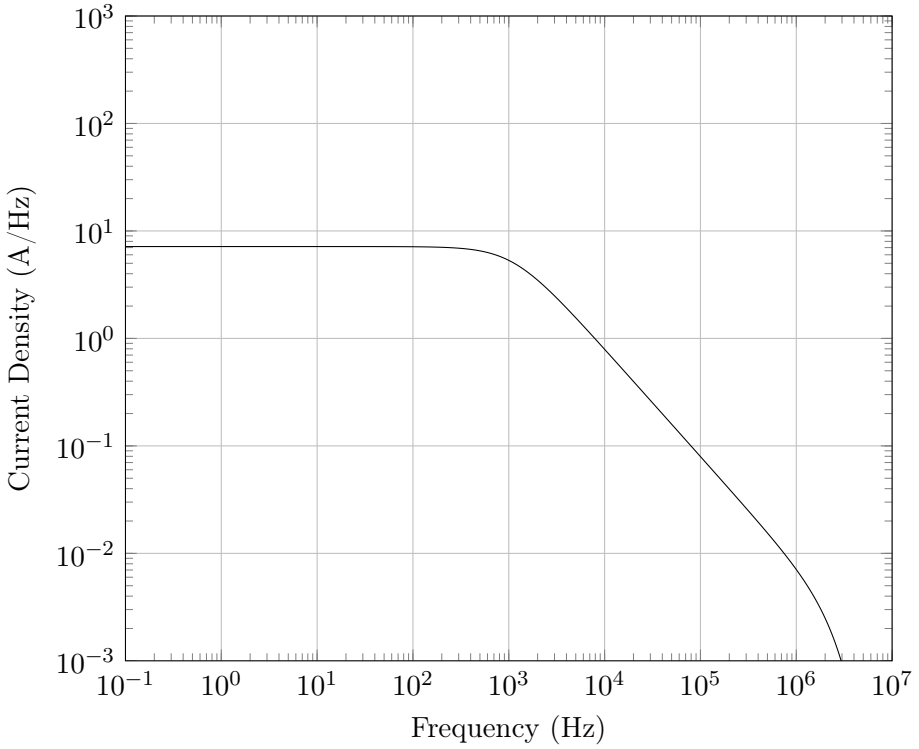


FIGURE 5.6: Current density of the approximation model produced from the waveshape plotted in *Figure 5.4*.

5.5 Conclusion

This chapter has discussed the experimental methodology. The results of the experiment are simulated and errors have been defined for the first and subsequent short strokes.

The following chapter utilises these results in order to draw conclusions about the viability of this approximation as a suitable replacement for the Heidler function in the IEC 62305-1 standard. Some comments about the further work that can be carried out are also made.

Chapter 6

Discussion and Further Work

This chapter critically analyses the results obtained in the previous chapter. The lightning stroke current is analysed, noting some features of the waveshapes of the approximation and the Heidler function. A method is shown for choosing the rise time constant in the approximation. The approximation is a good replacement for the Heidler function as it takes the same form and contains most of the same parameters. Some notes are made about the derivatives, in particular the effect that the subsequent short stroke can have on a system. An untested hypothesis about the error percentages is discussed. There is some discussion about the frequency response of the approximation with reference to the lightning protection standard. Comments are made about the further work that is required to optimise the approximation.

6.1 Overview

This chapter points out several observations and discusses any implications that they may have in using the approximation. Some conclusions about the validity of the approximation and the suitability as a replacement for the Heidler function are made. Some comments are made about the work that can be done to further this research.

6.2 Time Domain

As there is no accurate way of integrating the Heidler function and hence obtaining frequency domain information without numerical methods, the comparisons between the Heidler function and the approximation are made in the time domain. By using this

method, the maximum errors can be quantified. The following two sections discuss the results obtained in *Sections 5.3* and *5.4*.

6.2.1 Lightning Stroke Current

Chapter 5 discussed the first and subsequent stroke simulations in isolation of each other. Several observations are made about the two strokes together. From the graphs in *Figures 5.1* and *5.4*, it is obvious that the shape of the graph is the same for both waveshapes but with different time and amplitude scales. The decay parts of the approximation waveshapes follow the Heidler function decay exactly as expected. Any errors are only present in the rise part of the waveshapes.

The values of ω_0 (approximation rise time constant) and n_a (approximation steepness factor) that are used in creating the approximations shown in *Figures 5.1* and *5.4* are determined empirically. These values can be seen in *Tables 5.1* and *5.2* respectively. The IEC 62305-1 is used as a control in the evaluation of the approximation and it states that for the first and subsequent short strokes defined, a steepness factor, n_h, of 10 is required. It was found empirically that an n_a of 33 is appropriate for this case and therefore in this study only the rise time constant, ω_0, is increased for a faster rise time. This increase is expected as $\omega_0 \propto \frac{1}{t}$ and τ_1 (Heidler rise time constant) decreases with a quicker rise time. From the values in Table B.1 in the IEC 62305-1 standard, it is seen that the τ_1 ratio of the first stroke to the subsequent stroke is $19/0.454 = 41.85$. Looking at the same ratio of ω_0 with the values used in *Tables 5.1* and *5.2*, there is a ratio of $1\ 768\ 211/74\ 000\ 000 = 0.023895$. This is the inverse of 41.85 and therefore it is concluded that if the values of τ_1 are known and only one value of ω_0 is known, the known value of ω_0 can be multiplied or divided by the ratio of τ_1. Multiplication of ω_0 is done for a decrease in τ_1 and division for an increase in τ_1.

According to the IEC 62305-1 (Table C.3), the tolerance on peak current is $\pm 10\%$ for both first and subsequent strokes [1]. Similarly the tolerance on the rise time is $\pm 20\%$ for both the first and subsequent strokes. In order for an approximation to be a suitable replacement for the Heidler function, it must fit within these boundaries. *Table 6.1* shows the calculated peak current and rise time errors for both functions (Heilder and approximation) and both waveshapes (first and subsequent strokes). The errors for the first stroke are calculated as a percentage of a 10/350, 200 kA waveshape and the errors for the subsequent stroke are calculated as a percentage of a 0.25/100, 50 kA waveshape. It is clear from the table that the approximation is also well within the allowed tolerance and is therefore suitable as a replacement to the Heidler function.

TABLE 6.1: Comparison of the errors for the approximation and the Heilder function for both the first and subsequent strokes

		Approximation	**Heidler**
First Stroke	**Peak Current Error (%)**	0.43	0.31
	Rise Time Error (%)	2.46	0.19
Subsequent Stroke	**Peak Current Error (%)**	0.14	0.02
	Rise Time Error (%)	0.23	0.75

Another observation that is made is that the maximum absolute error in the first stroke is 1.38% and 1.36% in the subsequent stroke. This is a small change and it could be attributed to rounding errors when finding values of ω_0. This indicates that the maximum absolute error is constant for any approximation waveshape. This is unproven and is merely an observation but these errors do hold true for the waveshapes defined in the IEC 62305-1 standard which is set as the control in this study (see *Chapter 2*).

I_0 (peak current), η (peak current correction) and τ_2 (decay time constant) are the same for both the Heidler function and the approximation. This is expected as only $x_h(t)$ is replaced in the Heidler function with $x_a(t)$ in the approximation. As these are the respective rise time functions, it makes sense that the amplitude and decay time parts of the equation are unaffected. This implies that the approximation is easily interchangeable with the Heidler function.

Figures 6.1(a) and *6.1(b)* show the effects of changing the steepness factor, n_h, on the Heidler function and its first time derivative respectively. A steeper graph implies a faster rise time and hence the steepness factor affects the rise time of the waveshape, however the defining feature change is the steepness of the rise time. The half peak value remains at the same point in time for different steepness factors. The maximum instantaneous change in current occurs later in time and with a greater amplitude for a greater n_h. This occurs shortly after the first knee (the upward bend) in the curve.

Figures 6.1(c) and *6.1(d)* show the effects of changing the steepness factor, n_a, on the approximation and its first time derivative respectively. The change in the rise time of the waveshape is not as significant as with the Heidler function but the upward trend does still begin later in time. As expected, the maximum instantaneous change in current still occurs later in time but the peak value is decreased with an increase in n_a.

Figures 6.2(a) and *6.2(b)* show the effects of changing the rise time constant, τ_1, on the Heidler function and its first time derivative respectively. A smaller rise time constant produces a faster rise time of the waveshape and hence the steepness is also increased. The defining feature is the change in rise time. Again the peak instantaneous change in current occurs later in time with an increase in τ_1 but converse to what is seen with the steepness factor, the peak amplitude decreases.

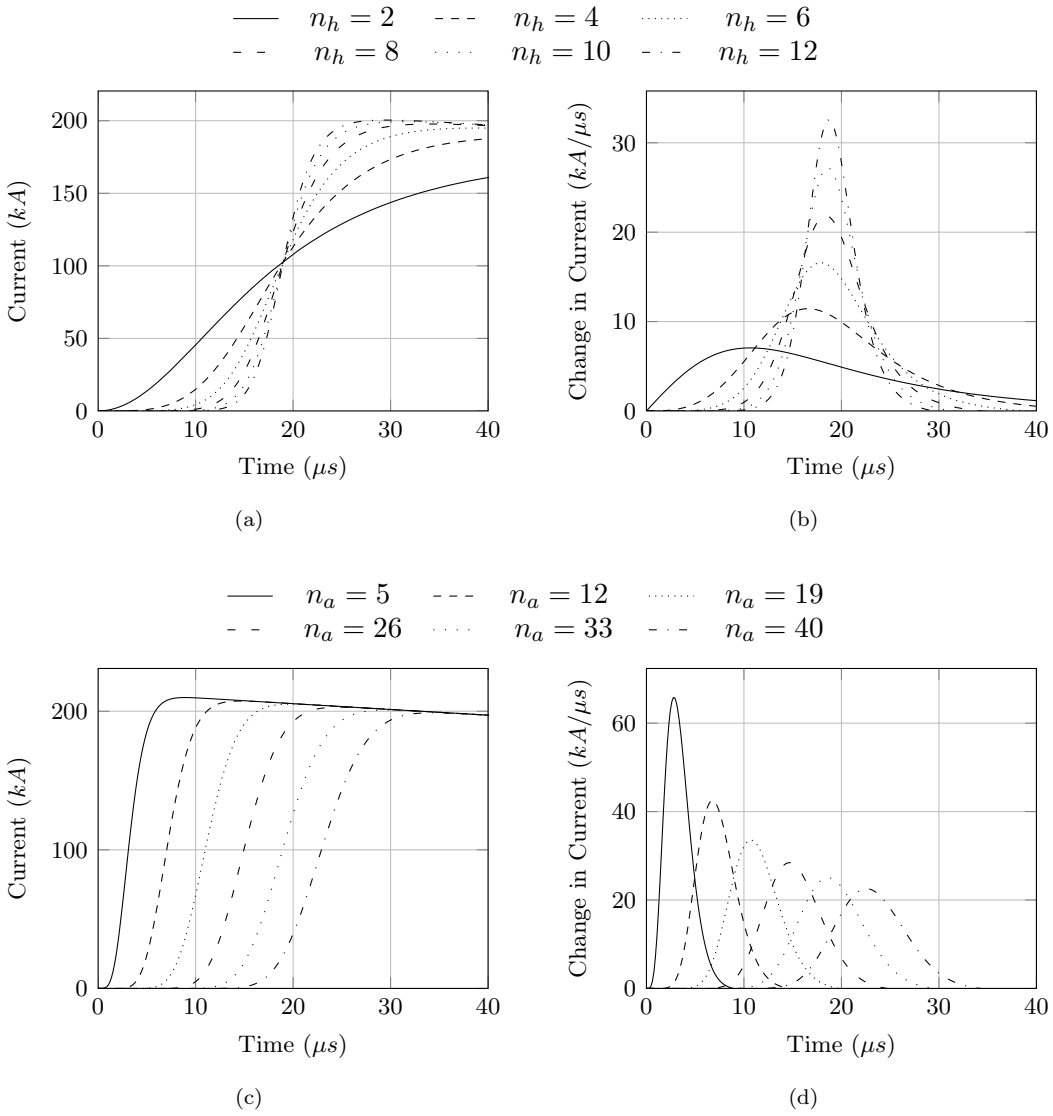


FIGURE 6.1: Effects of varying the steepness factors, n_h and n_a, in both the Heidler function and the approximation respectively. The (a) Heidler function and the (b) Heidler function derivative are compared to the (c) approximation and its (d) derivative.

Figures 6.2(c) and *6.2(d)* show the effects of changing the rise time constant, ω_0, on the approximation and its first time derivative respectively. A greater ω_0 results in a faster rise time. Again this affects the steepness of the rise time graph but the defining feature is the change in rise time. The derivative shows that the increase in ω_0 increases the amplitude of the peak instantaneous change in current however this occurs earlier in time unlike the other figures. ω_0 is proportional to the inverse of time ($\omega_0 \propto \frac{1}{t}$) and therefore the opposite of what is seen with the Heidler function (and τ_1) is expected with the approximation (and ω_0).

The steepness factors and the rise time constants of the Heidler function and the approximation do not have the same effect on their respective waveshapes and hence these

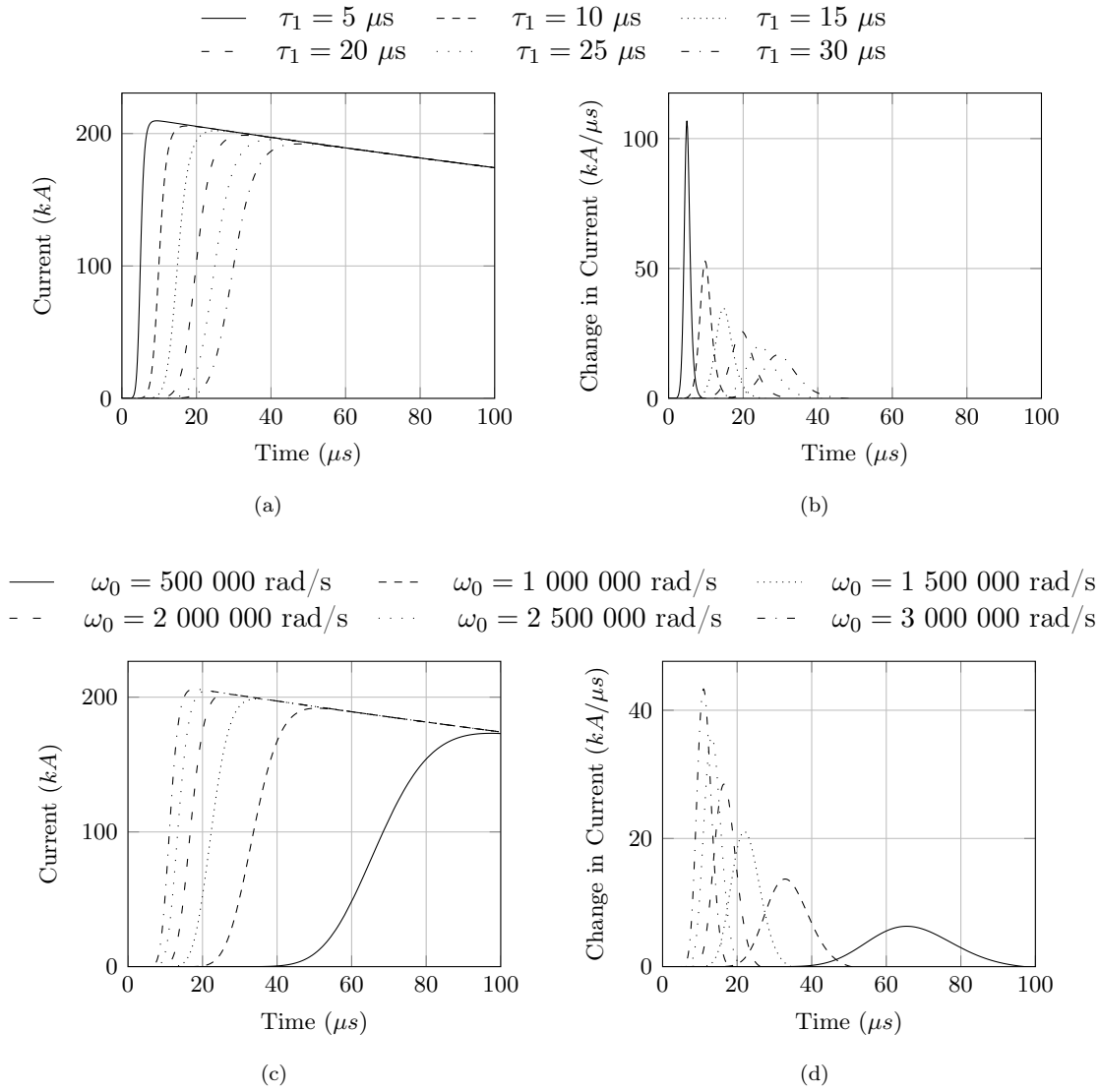


FIGURE 6.2: Effects of varying the rise time constants, τ_1 and ω_0, in both the Heidler function and the approximation respectively. The (a) Heidler function and the (b) Heidler function derivative are compared to the (c) approximation and its (d) derivative.

values for the approximation are calculated empirically. This method can be improved by finding some relationship between these parameters for the two functions (see *Section 6.4*).

6.2.2 Lightning Stroke Current Derivative

When looking at the waveshapes of the derivatives of the approximated waveforms compared with those of the Heidler function in *Figures 5.2* and *5.5*, a few observations can be made. The first is that the peak change in current is seen at about 50% of peak current value during the rise of the waveshape. This holds true for both the Heidler function

and the approximation. This is expected as the rise time function is an S-curve which is most steep in the middle of the rise.

From the two graphs, it can be seen that the maximum change in current in the subsequent stroke is ten times greater than that of the first stroke. This is critical when designing LPSs as the change in current is directly proportional to the voltage produced across an inductor (any wire). Therefore, the subsequent short strokes are more likely to have an effect on more sensitive systems due to even the smallest inductances.

As discussed above, the difference in the errors in the first short stroke and the subsequent short stroke is almost the same. The maximum absolute error in the first stroke is 7.91% and 7.86% in the subsequent stroke. This could once again be attributed to rounding errors. This further indicates that the maximum absolute error could be constant for any approximation waveshape. However this is still merely a hypothesis and would require further simulation and verification.

6.3 Frequency Domain

One of the reasons for undertaking this study is to obtain an analytical Fourier transform for the Heidler function (see *Chapter 2*). This implies that any transform of the Heidler function is done numerically which has inherent errors. There is no real way to quantify the error of the approximation in the frequency domain. *Figure 6.3* shows an adaptation of Figure B.5 in the IEC 62305-1 standard with the results obtained from the Fourier transform of the approximation (*Equation 4.13*) plotted on top. Line 2 shows the expected amplitude density of the first short stroke current while line 3 shows the expected amplitude density of the subsequent short stroke current. The results from the approximation clearly follow their respective waveshape expectations.

A current amplitude density is chosen because that is what is stipulated in the standard. Clearly, if the values are multiplied by their respective frequencies i.e. *Equation 4.13* is multiplied by frequency, the amplitude spectrum can be found. It is clear that for the first short stroke the peak current components are between about 500 Hz and 40 kHz with a rapid decay above 40 kHz. The subsequent short stroke has lower amplitude current components with a wider frequency range as expected. The peak current components here are between about 1 kHz and 1 MHz. The subsequent short stroke is more important when analysing wideband or high frequency systems/effects.

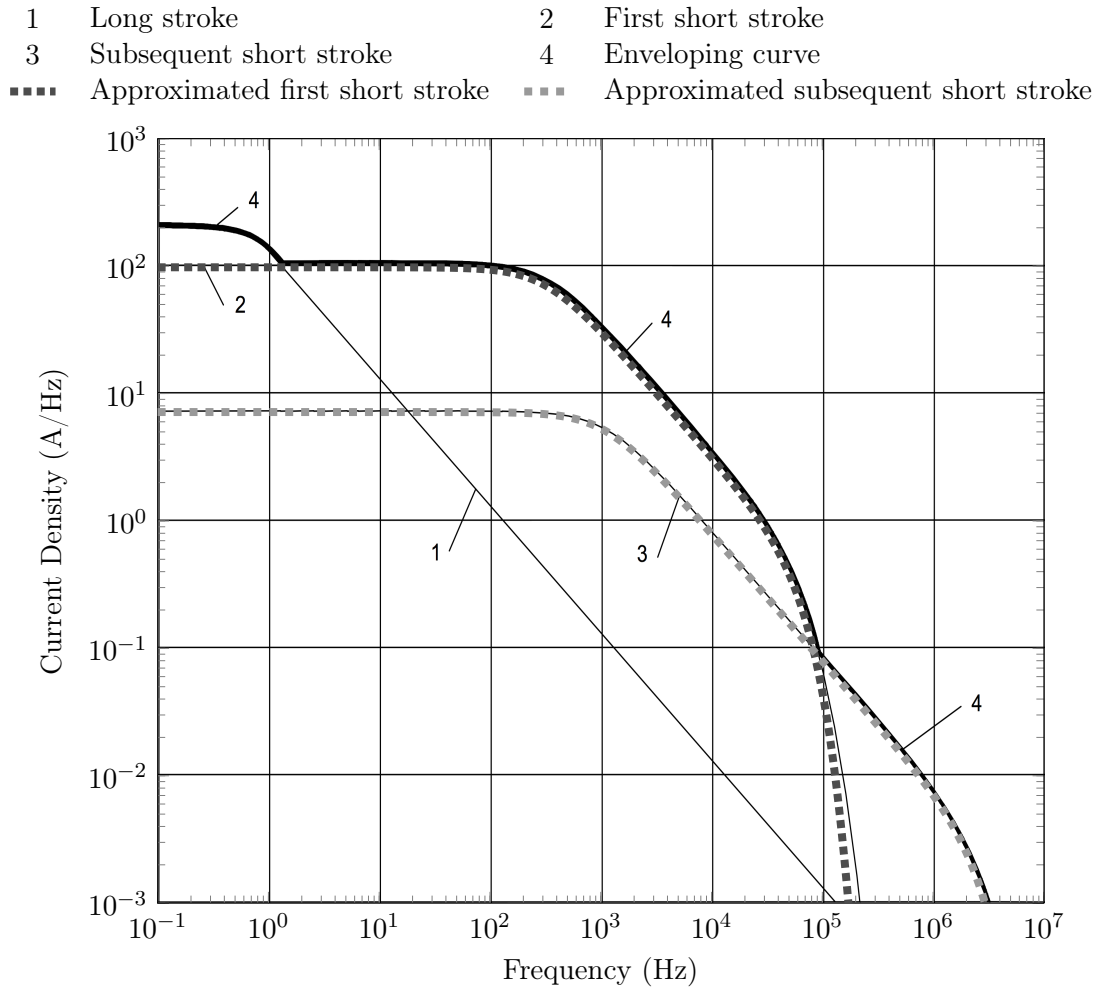


FIGURE 6.3: Amplitude densities of the different lightning currents according to LPL-I as stipulated by the IEC 62305-1 with the results of the Fourier transform of the approximation (adapted from Figure B.5 in [1]). The numbers point to the solid lines obtained from the standard.

6.4 Further Work

This study provides a replacement for the Heidler function that can be integrated. There is enough evidence given via experimentation (simulation) to define a suitable function that can be used. The evidence in this study is based on the waveforms and information outlined in the standard. However there are areas that can be further evaluated to possibly optimise the use of this function.

As noted above there is an error associated with the current waveshape and its derivative when compared with those of the Heidler function. This error is within a tolerable range and is quantified. It can therefore be taken into account in very sensitive system designs. It is posited above that this error could be consistent across all variations of the waveshape, however there are only two cases dealt with in this study (the only two

waveshapes detailed in the IEC 62305-1) and therefore this hypothesis requires further testing.

Another area for further research is again related to the errors that are quantified above. It is possible that the errors are as "high" as they are (no approximation will ever have zero error) because the numbers used for n_a (approximation steepness factor) and ω_0 (approximation rise time constant) are determined empirically. These could be better calculated by using some form of error optimisation algorithm. With these calculated numbers the error could be reduced.

There may be some relationship between ω_0 and the parameters used in the Heidler function, particularly τ_1 (Heidler rise time constant). By the same notion there may be some relationship between n_a and the parameters used in the Heidler function. These relationships would make plotting different waveshapes even easier than using the ratio method described in *Section 6.2.1* above. Further work is required to find such relationships. This however does not affect the validity of the approximation as a suitable replacement for the Heidler function with an analytical integral.

6.5 Conclusion

This chapter has critically analysed the results obtained in the previous chapter. It has drawn some conclusions about these results and hence the viability of the approximation. Some further work is posited to further optimise the approximation and lower the error.

The following chapter concludes this dissertation by summing up all the work that has been discussed and stating the conclusions that are drawn.

Chapter 7

Conclusion

An approximation to the Heidler function that has an analytical integral has been developed and discussed. This is useful in situations where the EM fields produced by a lightning stroke need to be calculated. It is also useful in any scenario where the frequency components of a lightning stroke are required for evaluation. The properties of the approximation are discussed with reference to the IEC 62305-1 standard. The viability of the approximation as a suitable replacement for the Heidler function in the standard have been evaluated through the investigation of the simulations produced. As the study is based on the guidelines in the IEC lightning protection standard, the lightning strokes defined therein are the ones used for the evaluation of viability.

It can be seen that the waveshapes produced by the approximation are very similar to those produced by the Heidler function. The maximum error in amplitude for the first and subsequent lightning stroke currents is less than 1.5%. The maximum error in the derivative is however greater but still less than 8%. This is still within the parameters defined in the standard which are based on some of the original lightning current analyses. The simulations detail the frequency response of the approximation for both waveshapes. There is no way of quantifying the error in this result because the Heidler function has no analytical integral and hence no Fourier transform. However the results are similar to what is expected in the lightning protection standard. All of this provides evidence that this approximation is a suitable replacement for the Heidler function when integrals and frequency spectra of lightning strokes are required.

The approximation has been designed using the Heidler function as a base and therefore they are easily interchangeable. When breaking the functions into components, the only difference is in the rise time functions. Other than that the two equations contain the same parameters. There is a ratio for the rise time constant that is found for different waveshapes of the Heidler function. The inverse of this ratio holds true for

the approximation giving further evidence of the consistency across the two functions. Therefore the approximation can easily be used in place of the Heidler function taking into account the quantified error (if necessary).

Additional work is required to optimise the approximation. This would further reduce the error and make working with the approximation even easier. This work includes proving or disproving the hypothesis that the error remains constant for any waveshape produced by the approximation. There is only an empirical optimisation of the parameters used in this study. A full optimisation algorithm should be run in order to reduce the 1.5% inaccuracy between the approximation and the Heidler function. It is posited that there may be some relationship between the parameters used in the Heidler rise time function and the approximation rise time function. Finding this relationship would further simplify the use of the approximation in studies and system design.

The approximation that is developed is found to be a suitable replacement for the Heidler function with the errors quantified and an analytical integral. Evidence is provided to show that the approximation to the Heidler function developed in this dissertation, can be used for the first and subsequent short strokes mentioned in the IEC 62305-1 with less than 1.5% error.

Appendix A

Approximation to the Heidler Function - Development

A.1 Overview

The process of developing an approximation to the Heidler function is easily described in a few steps. This appendix goes into more detail and shows all the necessary steps in developing the approximation.

A.2 Developing the Approximation

Equation A.1 shows the Heidler rise time function and it is clear that this function cannot be analytically integrated.

$$x_h(t) = \frac{\left(\frac{t}{\tau_1}\right)^{n_h}}{1 + \left(\frac{t}{\tau_1}\right)^{n_h}} \tag{A.1}$$

A plot of this is seen in *Figure A.1* (an S-curve).

The S-curve rises to a value of one and remains constant. It is clear from this that a step response is required. The approximation rise time function can be defined as in *Equation A.2*.

$$X_a(s) = \frac{1}{s} H(s) \tag{A.2}$$

Where:

$H(s)$ = Transfer function (Laplace domain)

$\frac{1}{s}$ = Unit step function in the Laplace domain

The step response of an n-th order real and negative pole in the Laplace domain produces

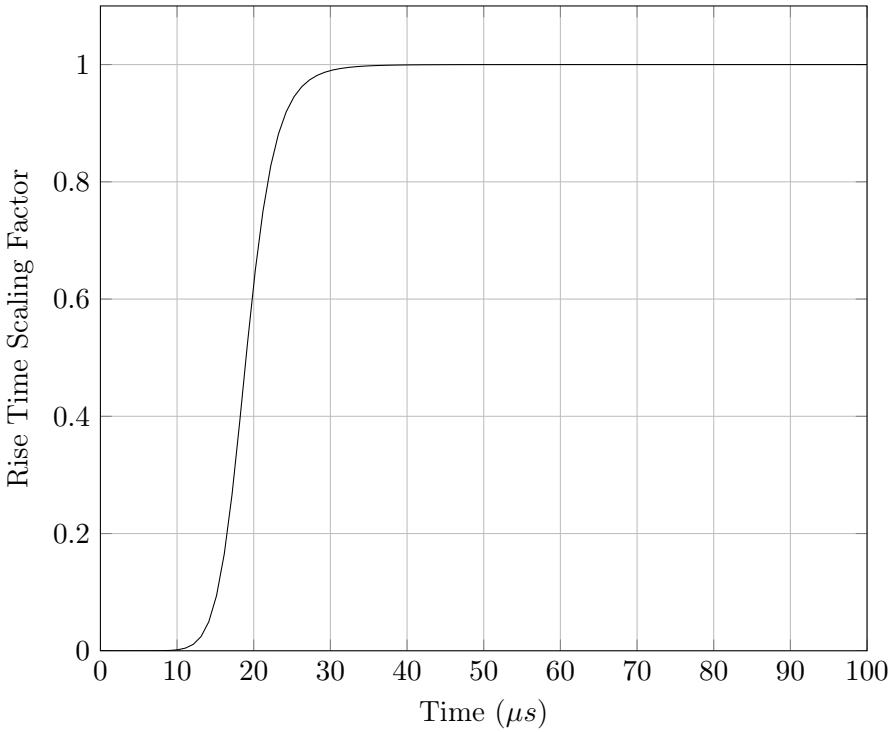


FIGURE A.1: Graph depicting the rise function of the Heidler function (an S-curve).

an S-shaped curve response in the time domain. Therefore the transfer function can be defined as in *Equation A.3*.

$$H(s) = \frac{1}{\left(\frac{s}{\omega_0} + 1\right)^{n_a}} \tag{A.3}$$

Where:

ω_0 = Some real and negative value

By substitution, *Equation A.2* becomes *Equation A.4*.

$$X_a(s) = \frac{1}{s} \frac{1}{\left(\frac{s}{\omega_0} + 1\right)^{n_a}} \tag{A.4}$$

The time domain equation is required which can be found by taking the inverse Laplace transform of *Equation A.4* as defined in *Equation A.5*.

$$\begin{aligned} x_a(t) &= \mathcal{L}^{-1}\{X_a(s)\} \\ &= \mathcal{L}^{-1}\left\{\frac{1}{s}\frac{1}{\left(\frac{s}{\omega_0} + 1\right)^{n_a}}\right\} \\ &= 1 - e^{-\omega_0 t}\left(\sum_{i=0}^{n_a} \frac{\omega_0^i t^i}{i!}\right) \end{aligned} \tag{A.5}$$

By substituting this back into the generalised form of the lightning stroke current shown in *Equation A.6*, the complete approximation can be seen in *Equation A.7*.

$$i_a(t) = \frac{I_0}{\eta} x_a(t)\, y(t) \tag{A.6}$$

$$= \frac{I_0}{\eta}\left(1 - e^{-\omega_0 t}\left(\sum_{i=0}^{n_a} \frac{\omega_0^i t^i}{i!}\right)\right) y(t)$$

$$= \frac{I_0}{\eta}\left(1 - e^{-\omega_0 t}\left(\sum_{i=0}^{n_a} \frac{\omega_0^i t^i}{i!}\right)\right) e^{-t/\tau_2} \tag{A.7}$$

A.3 Conclusion

This appendix provides all the mathematical steps required to develop the approximation to the Heidler function. This starts at the step response function and goes through until the final equation.

Appendix B

Initial Findings Using the Approximation

B.1 Preamble

This appendix is a paper that was accepted and presented for publication by the International Conference on Lightning Protection (ICLP) in 2014, hosted in Shanghai, China. The paper is entitled: ***Developing an Approximation to the Heidler Function - With an Analytical Transformation into the Frequency Domain***.

B.2 Paper Description

This paper discusses the preliminary development of the approximation to the Heidler function. It also shows the preliminary results obtained from simulations of the approximation. These results are without any optimisation.

These preliminary results indicated that this approximation is very promising and allowed for further research to optimise the function. The frequency results obtained broadened the scope of the approximation that was developed.

2014 International Conference on Lightning Protection (ICLP), Shanghai, China

Developing an Approximation to the Heidler Function - With an Analytical Transformation into the Frequency Domain

Brett R. Terespolsky and Ken J. Nixon
School of Electrical and Information Engineering
University of the Witwatersrand
Johannesburg, South Africa
Email: bteres@ieee.org

***Abstract*—IEC 62305 utilises the Heidler function as the standardised lightning current waveshape because it mimics the properties of a real lightning stroke. There is no analytical solution to the integral of the Heidler function and this means that it is not possible to obtain an expression for the Heidler function in the frequency domain. There are several approximations that are used to overcome this shortcoming. This paper proposes a new approximation that is designed in the Laplace domain. Initial results show that the amplitude differs with that of the Heidler function by no more than 3.7%. Furthermore, the first derivative of the approximated current waveshape, dI/dt, differs with that of the Heidler function by 10.5%. This however can be explained by the steepness factor not being calibrated correctly for the same shape Heidler function. The approximation is created in the Laplace domain and therefore it is trivial to plot the frequency spectrum of the approximation. Frequency analysis shows that the approximation agrees with those of other researchers. It is concluded that the initial results are evident of a promising approximation to the Heidler function.**

***Index Terms*—Lightning Channel Base Current; LEMP; IEC 62305; Heidler; Laplace; Frequency Domain; Approximation.**

I. Introduction

Lightning current data studies have shown that although lightning currents have random waveshapes, there are certain characteristics that each lightning current has [1]–[3]. IEC 62305 defines these characteristics for different types of lightning strokes. In order to simulate the behaviour of a lightning stroke, the standard recommends the use of the Heidler function as it meets the criteria outlined in the standard [4].

This function is ideal for current amplitude and other parameters in the time domain such as the charge and change in current. There is however no analytical transform of the Heidler function into the frequency domain because it cannot be integrated. This leads to problems when trying to obtain an accurate power spectral density plot of a particular lightning current. With a power spectral density plot, it is possible to analyse the effects of particular frequencies on a system. Furthermore, the integral of a lightning channel base current is required when carrying out Lightning Electromagnetic Pulse (LEMP) calculations. Having a function that has an analytical expression to its integral simplifies these LEMP calculations [5].

Therefore an approximation to the Heidler function that is transformable into the frequency domain is proposed. This can be used to show the effects of lightning current frequency components on systems.

This paper details the process of developing such an approximation by first detailing some background into the use of the Heidler function and its limitation with respect to Laplace/Fourier transform. Next, the Laplace domain approximation is developed and some preliminary results are given to show the viability of the approximation. Finally, the direction of the work is outlined and the paper is concluded.

II. Background

The IEC standard on Lightning Protection, IEC 62305, discusses different types of lightning currents such as a first return stroke, subsequent strokes, etc. [4]. In this standard the shape of a typical lightning stroke is described along with properties (of a lightning current) that must be used in the design of lightning protection systems. An adaptation of the waveshape shown in IEC 62305 standard is shown in Figure 1 [4]. This figure shows how the different stroke currents, such as the 1.2/50, 8/20 and 10/350 are composed. T_1 is the rise time (number before the '/') and T_2 is the fall time (number after the '/'). It is important that any lightning current shape can be obtained in order to test against different scenarios and lightning protection levels. Therefore the Heidler function is used in the IEC 62305 because it contains different factors allowing for the rise time, fall time, amplitude and steepness factors to be customised.

The Heidler function is defined as in *Equation 1* [3]

$$i(t) = \frac{I_0}{\eta} \frac{\left(\frac{t}{\tau_1}\right)^n}{1 + \left(\frac{t}{\tau_1}\right)^n} e^{-\frac{t}{\tau_2}} \tag{1}$$

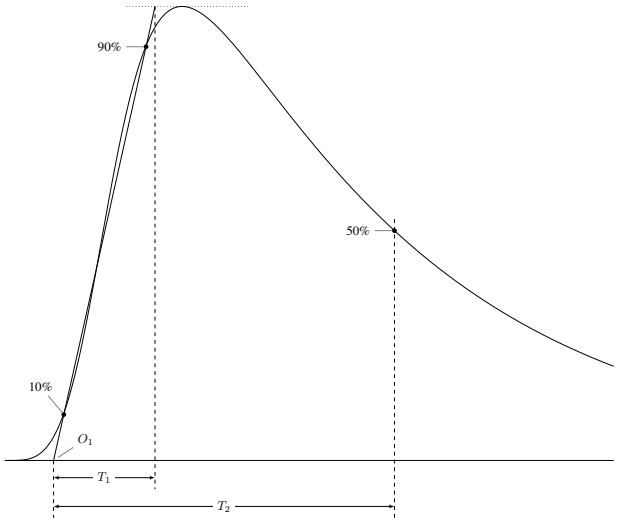


Fig. 1. Definitions of short stroke parameter adapted from [4]

Where:

I_0 = Peak current [kA]

η = Correction factor of peak current

τ_1 = Rise time constant [s]

τ_2 = Fall time constant [s]

n = Steepness factor

Equation 1 is often written as $i(t) = \frac{I_0}{\eta} x(t)y(t)$. Where $x(t)$ and $y(t)$ are the rise and fall equations represented in *Equations 2* and *3* respectfully.

$$x(t) = \frac{\left(\frac{t}{\tau_1}\right)^n}{1 + \left(\frac{t}{\tau_1}\right)^n} \tag{2}$$

$$y(t) = e^{-\frac{t}{\tau_2}} \tag{3}$$

Equation 3 is the decay function and can be integrated. Therefore this function is left as is in the approximation. Furthermore, the constant, $\frac{I_0}{\eta}$ can also be included directly in the approximation. *Equation 2* on the other hand, is an S-curve and the steepness of the rise as well as the front duration of waveshape can be adjusted by modifying n and τ_1 respectfully. This allows for a configurable rise time and maximum dI/dt.

The rise time equation in *Equation 2* cannot be transformed analytically (using Laplace or Fourier transforms) into the frequency domain because it cannot be integrated [6]. This creates a problem when accurate analyses of the frequency components of a lightning strike are required. For example, if the amplitude of the 11 kHz component of a lightning stroke is required to evaluate if lightning would introduce noise into a system operating at 11 kHz, it would not be possible to plot an analytical power spectral density from the Heidler function.

Furthermore, the numerical analysis of the LEMP fields is related to the lightning channel base current. This can be seen in *Equation 4*

$$i(z',t) = u(t - z'/v_f)P(z')i(0, t - z'/v) \tag{4}$$

where $i(z',t)$ is the return stroke current and $i(0, t - z'/v)$ is the lightning channel base current. In order to obtain the vertical and horizontal electric fields, $i(z',t)$ is integrated when solving Maxwell's equations. When carrying out these calculations, the use of an equation with an analytical solution in the frequency domain is preferred as this simplifies the mathematics [5].

Because of these limitations, several researchers have tried to approximate the transform of the Heidler function [6]. Most of these approximations have one or another limiting factor that changes the Heidler function enough so that it is no longer highly customisable: not all of the parameters remain variable. Many approximations are for a set steepness factor or entire waveshape [6]. In [6], the authors create an approximation that can be used with any factors but it is extremely complex.

Another example is where Delfino et al in [7] describe how the lightning channel base current can be approximated in terms of a Prony series. The limitation with this approach is the large amount of computation required for each approximation.

Therefore the purpose of this research is to formulate a lightning channel-base current function that has "customisable" parameters and can be transformed analytically into the frequency domain for use in frequency design and analysis as well as LEMP calculations. The approximation is simple to use and understand. It is also closely related to the Heidler function and so most of the parameters stay the same and the structure of the equation is the same (i.e. $i(t) = \frac{I_0}{\eta} x(t)y(t)$). This function is approximating the Heidler function and the parameters outlined in the IEC 62305 and therefore any errors are with respect to the Heidler function.

III. Heidler Function Approximation

A different approach is taken to approximate the Heidler function. A transfer function is defined in the Laplace domain and then an inverse Laplace transform is carried out to obtain the Heidler function approximation. With this approach, the equation is already in the frequency domain and therefore an analytical transform is no longer required.

A. Creating the Heidler Function Approximation

The Heidler function is not analytically transformable into the frequency domain because of the rise function, $x(t)$ in *Equation 2.* This function is merely an S-curve and therefore the step response of an n-th order, real and negative, pole is used to approximate this part of the function. The start of the approximation is seen in *Equation 5.*

$$X(s) = \frac{1}{s\left(\frac{s}{\omega_0} + 1\right)^n} \tag{5}$$

Where:

ω_0 = Rise time constant (rad/s)

n = Steepness factor

By varying the values of n and ω_0, the shape of the S-curve that is produced by the inverse Laplace transform of *Equation 5* can be "customised". The inverse Laplace transform of *Equation 5* can be seen in *Equation 6*.

$$x(t) = 1 - e^{-\omega_0 t}\left(\sum_{i=0}^{n}\frac{\omega_0^i t^i}{i!}\right) \tag{6}$$

The Heidler function also has a decay function as shown in *Equation 3*. There is no need to modify this function as it behaves exactly as required and is analytically transformable into the frequency domain. By including the constant and the decay function from *Equation 1* in *Equation 6*, the complete time domain approximation is obtained as in *Equation 7*

$$i(t) = \frac{I_0}{\eta}\left(1 - e^{-\omega_0 t}\left(\sum_{i=0}^{n}\frac{\omega_0^i t^i}{i!}\right)\right)e^{-t/\tau_2} \tag{7}$$

where I_0, η and τ_2 are the same as those in the Heidler function.

Equation 8 shows the complex shifting property of the Laplace transform.

$$\mathcal{L}\left\{e^{-at}f(t)\right\} = F(s+a) \tag{8}$$

By applying this property to *Equation 5* and using *Equation 3* as the model, an overall approximation to the Heidler function in the frequency domain can be obtained, as shown in *Equation 9*. The constants I_0 and η have also been included in *Equation 9* as they are real constants and are only required for changing the peak amplitude of the impulse current.

$$I(s) = \frac{I_0}{\eta}\frac{1}{s+\frac{1}{\tau_2}}\frac{1}{\left(\frac{s+\frac{1}{\tau_2}}{\omega_0}+1\right)^n} \tag{9}$$

B. Frequency Domain

As the function is developed in the Laplace domain, simply replacing the s with $j\omega$ in *Equation 9* gives rise to the frequency domain equation as seen in *Equation 10*.

$$I(j\omega) = \frac{I_0}{\eta}\frac{1}{j\omega+\frac{1}{\tau_2}}\frac{1}{\left(\frac{j\omega+\frac{1}{\tau_2}}{\omega_0}+1\right)^n} \tag{10}$$

This can be used directly in LEMP equations or the modulus and argument can be found and the power spectral density and phase of the lightning current can be analysed. Alternatively a bode plot of *Equation 9* can be plotted directly to obtain a frequency response.

IV. Results

There are several aspects of importance with this approximation.

1) The amplitude and other properties such as the derivative need to be comparable to the Heidler function.
2) The parameters outlined in the IEC62305 must be comparable to the approximation (intended as future research).
3) A frequency analysis must be carried out to show the frequency spectra of the function.

A. Comparison to Heidler

The proposed approximation is with respect to the Heidler function and therefore tested against it to determine accuracy of the approximation. The two aspects looked at in this paper are the amplitude of the current waveshape as well as the instantaneous derivative.

1) Amplitude: A 4 kA, 10/350 lightning current waveshape is used to test the approximation against the Heidler function. To obtain this current with both functions the parameters in *Table I* are used. It is clear that the parameters are similar

TABLE I
TABLE OF PARAMETERS USED IN CREATING EQUATIONS FOR *Figure 2*.

	Heidler	**Approximation**
τ_1 (μs)	19	-
τ_2 (μs)	485	485
n	10	33
ω_0 (rad/s)	-	1700000
I_0 (kA)	4	4
η	0.9341	0.9341

for the two functions with the notable differences being the steepness factor (n) and the rise time constants (τ_1 and ω_0). The reason for this is that the approximation's parameters are defined in the Laplace domain and this leads to the steepness factor having to be larger. Moreover, a number in rad/s is required for the approximation while the Heidler function expects a rise time constant in μs. However as the decay function as shown in *Equation 3* is unchanged, τ_2 is identical to that used in the Heidler function. Moreover, the shape of the rise function (S-curve) is the same as that of the Heidler function and therefore the same I_0 and η are used to achieve the required peak current.

Figure 2 shows the plots of both the Heidler function and the approximation with a 4 kA current and a 10/350 waveshape. The parameters used in the approximation are found by brute-force trial-and-error. The authors made some educated guesses and then optimised the values by hand until the curves looked very similar. A better method is required for this (see *Section VI*). The absolute value of the difference between the two functions shows that there is a maximum error of about 3.7% of the maximum amplitude of the Heidler waveshape.

2) Derivative: The derivative of a lightning current is important when determining the effects of inductive elements in a system. Therefore the approximation must represent a similar dI/dt graph to that of the Heidler function. *Figure 3* shows the first derivative of both the Heilder function and the approximation. There is a fairly large discrepancy in the peak values which reaches about 10.5%. This is a large error however the peak amplitude of the approximation function could be increased when carrying out these kinds of analyses. Moreover, this discrepancy results from the steepness factor being too small. This can be rectified by finding the correct correlation between the steepness factors of both functions (see *Section VI*).

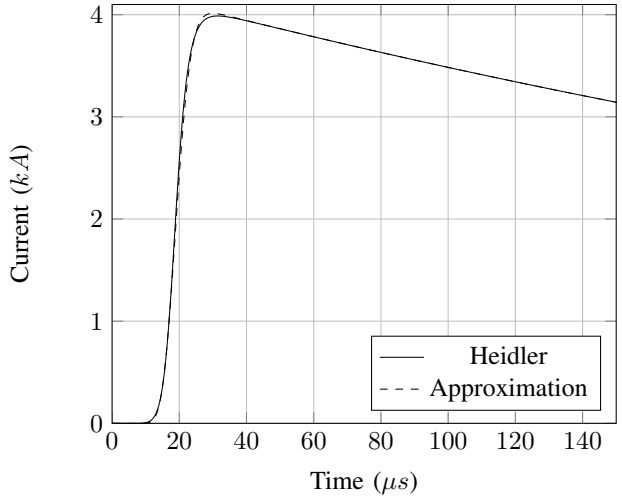


Fig. 2. Comparison between the approximation and the Heidler functions (tails shortened to show a more detailed comparison).

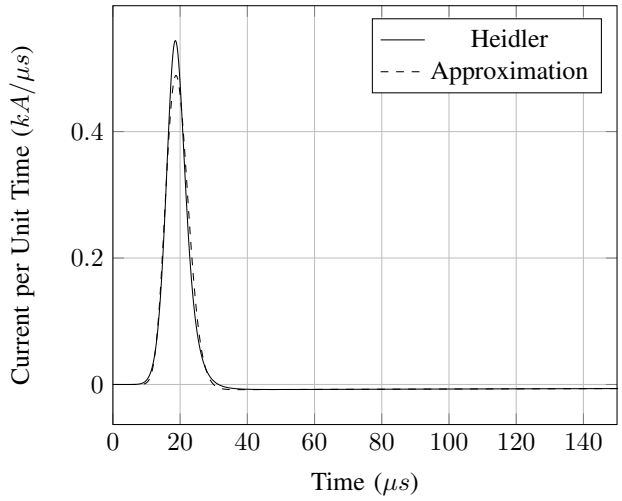


Fig. 3. Comparison between the first derivative of the approximation and the Heidler functions.

B. Frequency Analysis

A frequency analysis of lightning currents is useful to determine the effects that a particular frequency has on a system. Having a function that can be analytically transformed into the frequency domain allows for such an analysis. The power spectral density of the approximation can be plotted and hence the amplitude of the lightning current at a specific frequency can be determined.

Furthermore, having an expression for the lightning channel base current that is integrate-able is useful for carrying out LEMP calculations. The approximation is developed in the Laplace domain and is therefore trivially transformed into the frequency domain ($s = j\omega$) as expressed in *Equation 10*.

Preliminary analysis of the approximation in the frequency domain gives rise to the bode plot seen in *Figure 4*. The results

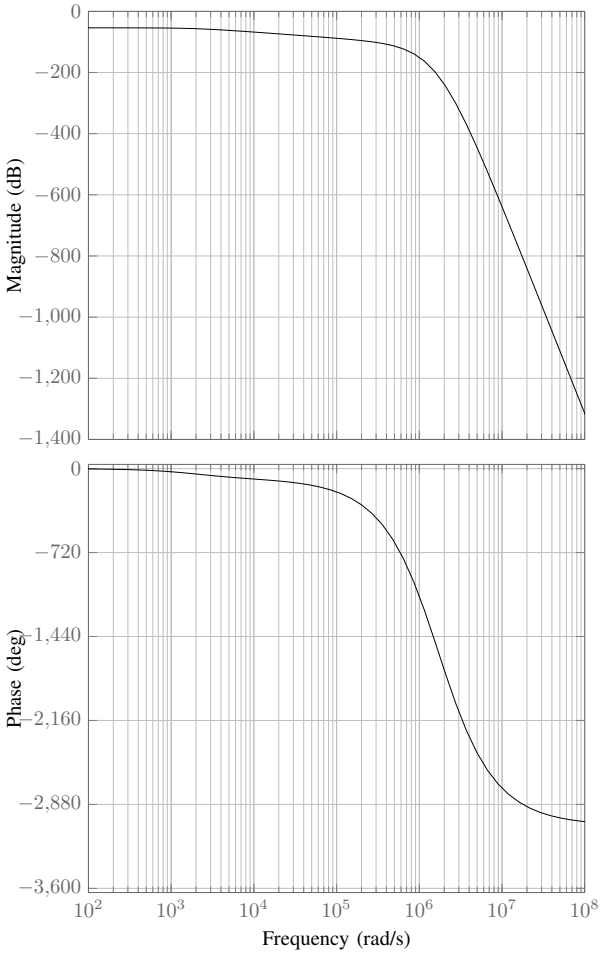


Fig. 4. Bode plot of the Heidler function approximation.

thus far look promising as they are aligned with the work done by Vujevic et al in [6] and [8] as well as that of Heidler et al in [9].

V. Discussion

This new proposed approximation to the Heidler function shows some promising preliminary results. Further work is required to fully understand how this function behaves with changing parameters (see *Section VI*).

The initial modelling has been carried out using a 4 kA, 10/350 lightning current waveshape. The parameters used in plotting the approximation are based on a trial-and-error brute-force process (see *Section III*). With these values the maximum error in the approximation with respect to the Heilder function is 3.7%. This is an acceptable error percentage in most engineering applications. However the instantaneous change in current is as much as 10.5% inaccurate. This can be easily explained by the steepness factor being incorrect. Therefore some optimisation and design is required to make sure that the parameters used in the approximation are the correct ones for the shape of the Heidler function used.

Because the approximation is developed in the Laplace domain, an expression for the approximation in the frequency domain is obtained by substitution rather than calculation. The initial plot of the frequency spectra shows that this approximation agrees with previous research.

VI. Future Research

There are several analyses required to determine the validity of such an approximation. In future work, the areas to be focused on are:

1) Correlating the parameters to those of the Heidler function.
2) Carrying out analyses on different waveshapes (such as the 1.2/50 and 8/20).
3) Comparing the characteristics of the approximation with those outlined in the IEC 62305 standard.
4) Further frequency analyses.

The parameters used in the approximation are similar to those used in the Heidler function. τ_2, I_0 and η are the same for both functions. n and ω_0 in the approximation are utilised in the Laplace domain and therefore are not necessarily correlated with n and τ_1 of the Heidler function. Further work is required to determine whether or not there is a relationship between these parameters in the approximation and in the Heidler function. If there is no obvious relationship then a table of parameter values for common waveshapes should be obtained.

Moreover, analyses should be carried out on different waveshapes. The analysis in this paper is done by modelling a 4 kA, 10/350 lightning current waveshape. It is still necessary to determine whether or not this approximation holds value for other lightning current waveshapes with varying amplitudes.

In order to make sure that this function can be used and is compliant with the standards, further work is required to determine whether or not this approximation holds the same characteristics as those outlined by the IEC for lightning currents.

Finally, more work is required to determine the accuracy of the power spectral density of this approximation.

VII. Conclusion

Lightning current waveshapes are utilised in analyses that can vary from instantaneous current change to frequency analysis. It is therefore important to have a standardised lightning current waveshape that can be used to perform these analyses. The IEC endorses the Heidler function for this use and although it shares the characteristics with those of a typical lightning current, it is limited in that an analytical integral cannot be obtained. An integral of such a function could be required in any scenario where an analysis is required on the frequency components of a lightning current or the effects thereof on a particular system. It is also required in calculating electric fields in LEMP analyses. Therefore approximations have been proposed throughout the years to solve this problem. No one approximation is perfect as all of them are limited in one or another aspect. Therefore another approximation is proposed that is developed in the Laplace domain, alleviating the need to transform into the frequency domain by taking the integral of the function.

This new approximation shows that it does a good job of approximating the Heidler function in the time domain. It also has characteristics (such as dI/dt) that are similar to the Heidler function. An initial frequency analysis shows that the approximation gives a similar frequency response to that of other researchers.

Acknowledgement

The authors would like to thank CBI-electric for funding the Chair of Lightning at the University of the Witwatersrand and for direct support of the Research Group and Eskom for the support of the Lightning/EMC Research Group through the TESP programme. Thanks are extended to the department of Trade and Industry (DTI) for THRIP funding as well as to the National Research Foundation (NRF) for direct funding of the Research Group.

References

[1] R. Anderson and A. Eriksson, "Lightning Parameters for Engineering Application," *Electra*, vol. 69, pp. 65–102, 1980. [Online]. Available: http://scholar.google.com/scholar?hl=en&btnG=Search&q=intitle:Lightning+Parameters+for+Engineering+Application#0

[2] K. Berger, R. B. Anderson, and H. Kroninger, "Parameters of Lightning Flashes," *Electra*, vol. 41, pp. 23–37, 1975.

[3] V. A. Rakov and M. A. Uman, *Lightning: Physics and Effects*. Cambridge University Press, 2003.

[4] IEC, *Protection against lightning - Part 1: General principles*, IEC Std. IEC 62 305-1, 2006.

[5] Z. Feizhou and L. Shanghe, "A new function to represent the lightning return-stroke currents," *IEEE Transactions on Electromagnetic Compatibility*, vol. 44, no. 4, pp. 595–597, Nov. 2002. [Online]. Available: http://ieeexplore.ieee.org/lpdocs/epic03/wrapper.htm?arnumber=1076024

[6] S. Vujević and D. Lovrić, "Exponential approximation of the Heidler function for the reproduction of lightning current waveshapes," *Electric Power Systems Research*, vol. 80, no. 10, pp. 1293–1298, Oct. 2010. [Online]. Available: http://linkinghub.elsevier.com/retrieve/pii/S0378779610001033

[7] F. Delfino, R. Procopio, M. Rossi, and F. Rachidi, "Prony Series Representation for the Lightning Channel Base Current," *IEEE Transactions on Electromagnetic Compatibility*, vol. 54, no. 2, pp. 308–315, Apr. 2012. [Online]. Available: http://ieeexplore.ieee.org/lpdocs/epic03/wrapper.htm?arnumber=5970112

[8] S. Vujevic, D. Lovric, and Z. Balaz, "Numerical approximation of the lightning current function," in *The 17th International Conference on Software, Telecommunications and Computer Networks*, vol. 2, no. 4, 2009. [Online]. Available: http://ieeexplore.ieee.org/xpls/abs_all.jsp?arnumber=5306877

[9] F. Heidler and J. Cvetić, "A class of analytical functions to study the lightning effects associated with the current front," *European transactions on electrical power*, vol. 12, no. 2, pp. 141–150, 2002. [Online]. Available: http://onlinelibrary.wiley.com/doi/10.1002/etep.4450120209/abstract

References

[1] IEC, *Protection against lightning - Part 1: General principles*, IEC Std. IEC 62 305-1, 2006.

[2] Z. Feizhou and L. Shanghe, "A new function to represent the lightning return-stroke currents," *IEEE Transactions on Electromagnetic Compatibility*, vol. 44, no. 4, pp. 595–597, Nov. 2002. [Online]. Available: http://ieeexplore.ieee.org/lpdocs/epic03/wrapper.htm?arnumber=1076024

[3] F. Heidler and J. Cvetić, "A class of analytical functions to study the lightning effects associated with the current front," *European transactions on electrical power*, vol. 12, no. 2, pp. 141–150, 2002. [Online]. Available: http://onlinelibrary.wiley.com/doi/10.1002/etep.4450120209/abstract

[4] M. Paolone, F. Rachidi, A. Borghetti, C. A. Nucci, M. Rubinstein, V. A. Rakov, and M. A. Uman, "Lightning Electromagnetic Field Coupling to Overhead Lines: Theory, Numerical Simulations, and Experimental Validation," *IEEE Transactions on Electromagnetic Compatibility*, vol. 51, no. 3, pp. 532–547, 2009.

[5] V. A. Rakov and M. A. Uman, *Lightning: Physics and Effects*. Cambridge University Press, 2003.

[6] V. Rakov and F. Rachidi, "Overview of recent progress in lightning research and lightning protection," *IEEE Transactions on Electromagnetic Compatibility*, vol. 51, no. 3, pp. 428–442, 2009. [Online]. Available: http://ieeexplore.ieee.org/xpls/abs_all.jsp?arnumber=5061618

[7] Y. Baba and V. a. Rakov, "Electromagnetic models of the lightning return stroke," *Journal of Geophysical Research*, vol. 112, no. D04102, Feb. 2007. [Online]. Available: http://doi.wiley.com/10.1029/2006JD007222

[8] C. W. I. McAfee and K. J. Nixon, "Lightning return stroke modelling with reference to lightning electromagnetic fields," in *Southern African Universities Power Engineering Conference*, Johannesburg, 2015.

[9] A. Agrawal, H. Price, and S. Gurbaxani, "Transient Response of Multiconductor Transmission Lines Excited by a Nonuniform Electromagnetic Field," *IEEE Transactions on Electromagnetic Compatibility*, vol. EMC-22, no. 2, pp. 119–129, May 1980. [Online]. Available: http://ieeexplore.ieee.org/lpdocs/epic03/wrapper.htm?arnumber=4091352

[10] M. Uman, D. McLain, and E. Krider, "The Electromagnetic Radiation from a Finite Antenna," *American Journal of Physics*, vol. 43, pp. 53 – 58, 1975. [Online]. Available: http://fpgamac.org/images/b/b2/Uman_EmagRadAntenna_1975.pdf

[11] C. A. Nucci and F. Rachidi, *The Lightning Flash*, ser. Power Series 34, V. Cooray, Ed. Institute of Electrical Engineers, 2003.

[12] V. Javor and P. D. Rancic, "A Channel-Base Current Function for Lightning Return-Stroke Modeling," *IEEE Transactions on Electromagnetic Compatibility*, vol. 53, no. 1, pp. 245–249, Feb. 2011. [Online]. Available: http://ieeexplore.ieee.org/lpdocs/epic03/wrapper.htm?arnumber=5613925

[13] C. A. Nucci and F. Rachidi, *Lightning Protection*, ser. 58, V. Cooray, Ed. The Institute of Engineering and Technology, 2010.

[14] Y.-C. H. Lee, D. M. Rubin, and I. R. Jandrell, "Use of dielectric properties of human tissues in the analysis of lightning injuries," in *International Conference on Lightning Protection*, Shanghai, 2014, pp. 1012–1017.

[15] H. Wei, X. Ba-lin, and G. You-gang, "Analysis of the lightning waveshape," in *Radio Science Conference, 2004. Proceedings. 2004 Asia-Pacific*, Aug. 2004, pp. 627–630.

[16] R. Anderson and A. Eriksson, "Lightning Parameters for Engineering Application," *Electra*, vol. 69, pp. 65–102, 1980. [Online]. Available: http://scholar.google.com/scholar?hl=en&btnG=Search&q=intitle:Lightning+Parameters+for+Engineering+Application#0

[17] K. Berger, R. B. Anderson, and H. Kroninger, "Parameters of Lightning Flashes," *Electra*, vol. 41, pp. 23–37, 1975.

[18] D. Pavanello, F. Rachidi, V. Rakov, C. Nucci, and J. Bermudez, "Return stroke current profiles and electromagnetic fields associated with lightning strikes to tall towers: Comparison of engineering models," *Journal of Electrostatics*, vol. 65, pp. 316–321, May 2007. [Online]. Available: http://linkinghub.elsevier.com/retrieve/pii/S0304388606001215

[19] D. Lovrić, S. Vujević, and T. Modrić, "On the estimation of Heidler function parameters for reproduction of various standardized and recorded lightning current

waveshapes," *International Transactions on Electrical Energy Systems*, vol. 23, no. 2, pp. 290–300, Mar. 2013. [Online]. Available: http://doi.wiley.com/10.1002/etep.669

[20] F. Delfino, R. Procopio, M. Rossi, and F. Rachidi, "Prony Series Representation for the Lightning Channel Base Current," *IEEE Transactions on Electromagnetic Compatibility*, vol. 54, no. 2, pp. 308–315, Apr. 2012. [Online]. Available: http://ieeexplore.ieee.org/lpdocs/epic03/wrapper.htm?arnumber=5970112

[21] F. Heidler, W. Zischank, Z. Flisowski, C. Bouquegneau, and C. Mazzetti, "Parameters of lightning current given in IEC 62305-background, experience and outlook," in *International Conference on Lightning Protection*, no. June, Uppsala, 2008, pp. 1–22. [Online]. Available: http://www.iclp-centre.org/pdf/Invited-Lecture-3.pdf

[22] F. Heidler, J. Cvetic, and B. Stanic, "Calculation of lightning current parameters," *IEEE Transactions on Power Delivery*, vol. 14, no. 2, pp. 399–404, Apr. 1999. [Online]. Available: http://ieeexplore.ieee.org/lpdocs/epic03/wrapper.htm?arnumber=754080

[23] V. Javor, "New Functions for Representing IEC 62305 Standard and Other Typical Lightning Stroke Currents," *Journal of Lightning Research*, vol. 4, no. 1, pp. 50–59, Jul. 2012. [Online]. Available: http://benthamscience.com/open/openaccess.php?jlr/articles/V004/SI0049JLR/50JLR.htm

[24] W. Gautschi, "A Computational Procedure for Incomplete Gamma Functions," *{ACM} Transactions on Mathematical Software*, vol. 5, no. 4, pp. 466–481, Dec. 1979. [Online]. Available: http://doi.acm.org/10.1145/355853.355863

[25] V. Javor, "Fourier Transform Application in the Computation of Lightning Electromagnetic Field," in *Fourier Transform Applications*. InTech. [Online]. Available: http://cdn.intechopen.com/pdfs/36425/InTech-Fourier_transform_application_in_the_computation_of_lightning_electromagnetic_field.pdf

[26] S. Vujević, D. Lovrić, and Z. Balaz, "Numerical approximation of the lightning current function," in *The 17th International Conference on Software, Telecommunications and Computer Networks*, vol. 2, no. 4, 2009. [Online]. Available: http://ieeexplore.ieee.org/xpls/abs_all.jsp?arnumber=5306877

[27] S. Vujević and D. Lovrić, "Exponential approximation of the Heidler function for the reproduction of lightning current waveshapes," *Electric Power Systems Research*, vol. 80, no. 10, pp. 1293–1298, Oct. 2010. [Online]. Available: http://linkinghub.elsevier.com/retrieve/pii/S0378779610001033

[28] C. L. Phillips, J. M. Parr, and E. A. Riskin, *Signals, Systems, and Transforms*, 4th ed. Pearson Education, 2008.

[29] R. S. Burns, *Advanced Control Engineering*. Butterworth-Heinemann, 2001.

[30] B. R. Terespolsky and K. J. Nixon, "Developing an Approximation to the Heidler Function - With an Analytical Transformation into the Frequency Domain," in *International Conference on Lightning Protection*, vol. 1, no. 1, Shanghai, 2014, pp. 1134–1138.

[31] The MathWorks, Inc. (2013) MATLAB. Version 8.1.0.604 (R2013a). Natick, Massachusetts.

[32] Wolfram Research, Inc. (2014) Mathematica. Version 10.0. Champaign, Illinois.

[33] Maxima. (2014) Maxima, a Computer Algebra System. Version 5.34.1. http://maxima.sourceforge.net/. [Online]. Available: http://maxima.sourceforge.net/

Bibliography

Agrawal, A., Price, H., and Gurbaxani, S. (1980). Transient Response of Multiconductor Transmission Lines Excited by a Nonuniform Electromagnetic Field. *IEEE Transactions on Electromagnetic Compatibility*, EMC-22(2):119–129.

Anderson, R. and Eriksson, A. (1980). Lightning Parameters for Engineering Application. *Electra*, 69:65–102.

Baba, Y. and Rakov, V. a. (2007). Electromagnetic models of the lightning return stroke. *Journal of Geophysical Research*, 112(D04102).

Berger, K., Anderson, R. B., and Kroninger, H. (1975). Parameters of Lightning Flashes. *Electra*, 41:23–37.

Burns, R. S. (2001). *Advanced Control Engineering*. Butterworth-Heinemann.

Delfino, F., Procopio, R., Rossi, M., and Rachidi, F. (2012). Prony Series Representation for the Lightning Channel Base Current. *IEEE Transactions on Electromagnetic Compatibility*, 54(2):308–315.

Eloundou, R. and Singhose, W. (2002). Interpretation of Smooth Reference Commands as Input-Shaped Functions. In *Proceedings of the 2002 American Control Conference*, volume 6, pages 4948–4953. IEEE.

Elrodesly, K. (2010). *Comparison Between Heidler Function And The Pulse Function For Modeling The Lightning Return-Stroke Current*. PhD thesis, Ryerson University.

Feizhou, Z. and Shanghe, L. (2002). A new function to represent the lightning return-stroke currents. *IEEE Transactions on Electromagnetic Compatibility*, 44(4):595–597.

Gamerota, W. R., Elisme, J. O., Uman, M. A., and Rakov, V. A. (2012). Current Waveforms for Lightning Simulation. *IEEE Transactions on Electromagnetic Compatibility*, 54(4):880–888.

Gautschi, W. (1979). A Computational Procedure for Incomplete Gamma Functions. *{ACM} Transactions on Mathematical Software*, 5(4):466–481.

Heidler, F. and Cvetić, J. (2002). A class of analytical functions to study the lightning effects associated with the current front. *European transactions on electrical power*, 12(2):141–150.

Heidler, F., Cvetic, J., and Stanic, B. (1999). Calculation of lightning current parameters. *IEEE Transactions on Power Delivery*, 14(2):399–404.

Heidler, F., Zischank, W., Flisowski, Z., Bouquegneau, C., and Mazzetti, C. (2008). Parameters of lightning current given in IEC 62305-background, experience and outlook. In *International Conference on Lightning Protection*, number June, pages 1–22, Uppsala.

Hwang, C. (1997). Numerical modeling of lightning based on the traveling wave equations. *IEEE Transactions on Magnetics*, 33(2):1520–1523.

IEC (2006). Protection against lightning - Part 1: General principles.

Javor, V. Fourier Transform Application in the Computation of Lightning Electromagnetic Field. In *Fourier Transform Applications*. InTech.

Javor, V. (2012). New Functions for Representing IEC 62305 Standard and Other Typical Lightning Stroke Currents. *Journal of Lightning Research*, 4(1):50–59.

Javor, V. and Rancic, P. D. (2011). A Channel-Base Current Function for Lightning Return-Stroke Modeling. *IEEE Transactions on Electromagnetic Compatibility*, 53(1):245–249.

Jia, W. and Xiaoqing, Z. (2006). Double-exponential expression of lightning current waveforms. In *Asia-Pacific Conference on Environmental Electromagnetics (CEEM)*, pages 320–323, Dalian.

Kuo, F. F. (1966). *Network Analysis and Synthesis*. John Wiley & Sons, Inc.

Lee, Y.-C. H., Rubin, D. M., and Jandrell, I. R. (2014). Use of dielectric properties of human tissues in the analysis of lightning injuries. In *International Conference on Lightning Protection*, pages 1012–1017, Shanghai.

Liu, X. and Liu, D. (2010). The Lightning Current Measurement Based on Wavelet Transform. *Modern Applied Science*, 4(4):19–25.

Lovrić, D., Vujević, S., and Modrić, T. (2013). On the estimation of Heidler function parameters for reproduction of various standardized and recorded lightning current waveshapes. *International Transactions on Electrical Energy Systems*, 23(2):290–300.

Mahajan, S. (2010). *Street-fighting mathematics - The art of educated guessing and opportunistic problem solving*. The MIT Press.

Maxima (2014). Maxima, a Computer Algebra System. Version 5.34.1.

McAfee, C. W. I. and Nixon, K. J. (2015). Lightning return stroke modelling with reference to lightning electromagnetic fields. In *Southern African Universities Power Engineering Conference*, Johannesburg.

Meng, X., Zhou, B. H., Yang, B., and Zhu, K. E. (2012). Analysis on influence of tall tower on lightning current measurement. In *Asia-Pacific Conference on Environmental Electromagnetics (CEEM)*, pages 145–147, Shanghai. IEEE.

Napolitano, F. (2011). An Analytical Formulation of the Electromagnetic Field Generated by Lightning Return Strokes. *IEEE Transactions on Electromagnetic Compatibility*, 53(1):108–113.

Narita, T., Yamada, T., Mochizuki, A., Zaima, E., and Ishii, M. (2000). Observation of current waveshapes of lightning strokes on transmission towers. *IEEE Transactions on Power Delivery*, 15(1):429–435.

Nucci, C. A. and Rachidi, F. (2003). *The Lightning Flash*. Power Series 34. Institute of Electrical Engineers.

Nucci, C. A. and Rachidi, F. (2010). *Lightning Protection*. 58. The Institute of Engineering and Technology.

Okabe, S., Takami, J., Tsuboi, T., Ueta, G., Ametani, A., and Hidaka, K. (2013). Discussion on standard waveform in the lightning impulse voltage test. *IEEE Transactions on Dielectrics and Electrical Insulation*, 20(1):147–156.

Paolone, M., Rachidi, F., Borghetti, A., Nucci, C. A., Rubinstein, M., Rakov, V. A., and Uman, M. A. (2009). Lightning Electromagnetic Field Coupling to Overhead Lines: Theory, Numerical Simulations, and Experimental Validation. *IEEE Transactions on Electromagnetic Compatibility*, 51(3):532–547.

Pavanello, D., Rachidi, F., Rakov, V., Nucci, C., and Bermudez, J. (2007). Return stroke current profiles and electromagnetic fields associated with lightning strikes to tall towers: Comparison of engineering models. *Journal of Electrostatics*, 65:316–321.

Phillips, C. L., Parr, J. M., and Riskin, E. A. (2008). *Signals, Systems, and Transforms*. Pearson Education, fourth edition.

Rachidi, F. (2005). Modeling lightning return strokes to tall structures: recent developments. In *VIII International Symposium on Lightning Protection*, number November.

Rakov, V. and Rachidi, F. (2009). Overview of recent progress in lightning research and lightning protection. *IEEE Transactions on Electromagnetic Compatibility*, 51(3):428–442.

Rakov, V. A. and Uman, M. A. (2003). *Lightning: Physics and Effects*. Cambridge University Press.

Roberts, G. W. and Sedra, A. S. (1997). *SPICE*. Oxford University Press, second edition.

Sato, N. (1980). Discharge current induced by the motion of charged particles. *Journal of Physics D: Applied Physics*, 13:3–7.

Terespolsky, B. R. and Nixon, K. J. (2014). Developing an Approximation to the Heidler Function - With an Analytical Transformation into the Frequency Domain. In *International Conference on Lightning Protection*, volume 1, pages 1134–1138, Shanghai.

The MathWorks, Inc. (2013). MATLAB. Version 8.1.0.604 (R2013a).

Uman, M., McLain, D., and Krider, E. (1975). The Electromagnetic Radiation from a Finite Antenna. *American Journal of Physics*, 43:53 – 58.

Visacro, S. (2004). A representative curve for lightning current waveshape of first negative stroke. *Geophysical Research Letters*, 31(7).

Vujević, S. and Lovrić, D. (2010). Exponential approximation of the Heidler function for the reproduction of lightning current waveshapes. *Electric Power Systems Research*, 80(10):1293–1298.

Vujević, S., Lovrić, D., and Balaz, Z. (2009). Numerical approximation of the lightning current function. In *The 17th International Conference on Software, Telecommunications and Computer Networks*, volume 2.

Wei, H., Ba-lin, X., and You-gang, G. (2004). Analysis of the lightning waveshape. In *Radio Science Conference, 2004. Proceedings. 2004 Asia-Pacific*, pages 627–630.

Wolfram Research, Inc. (2014). Mathematica. Version 10.0.

Zhang, Q., Feng, J., and Geng, X. (2010). The simulation of the return stroke current waveform along with the lightning channel. In *Asia-Pacific International Symposium on Electromagnetic Compatibility*, pages 1486–1489.